J. Fluid Mech. (1989), *vol.* 204, *pp.* 31–56
Printed in Great Britain

Passage through the critical Froude number for shallow-water waves over a variable bottom

By J. KEVORKIAN AND J. YU
Department of Applied Mathematics, University of Washington, Seattle, WA 98195, USA

(Received 27 February 1988 and in revised form 5 December 1988)

We study the behaviour of shallow (of order $\delta \ll 1$) water waves excited by a small (of order $\epsilon \ll 1$) amplitude bottom disturbance in the presence of a uniform oncoming flow with either constant or slowly varying Froude number F. When $F^* \equiv |F-1|\epsilon^{-\frac{1}{2}} \gg 1$, the speed and free surface perturbations are of order $\nu = O(\epsilon)$; these grow to become of order $\epsilon^{\frac{1}{2}}$ if $F^* = O(1)$. Therefore, the asymptotic expansions of the solution for $\epsilon \to 0$ depend on the order of F^*. These expansions are constructed in a form which remains valid for times of order ν^{-1}; they are then matched to provide results which are also valid for all F. The analytic results exhibit the interesting effects of weak nonlinearities including the steepening of waves and eventual formation of bores if $\delta\nu^{-\frac{1}{2}} \ll 1$, the surface rippling due to dispersion if $\delta\nu^{-\frac{1}{2}} = O(1)$, the strong interaction of waves and the periodic generation of upstream-propagating solitary waves if $F^* = O(1)$, etc. All these results are confirmed by numerical integration of the governing equations.

1. Introduction

This paper concerns the asymptotic solution for small-amplitude waves in shallow water over a variable bottom. We study in detail the special case of flow due to an isolated small (of order $\epsilon \ll 1$) bottom disturbance corresponding to a bump of fixed shape set impulsively into motion at either a constant or slowly varying dimensionless speed F (Froude number). Here, we define H to be the constant initial depth away from the bottom disturbance, δ to be the ratio of H to L, a characteristic wavelength of the flow, ϵ to be the ratio of the maximum bottom height A to H, and the Froude number F to be the ratio of $U_{-\infty}$, the uniform flow speed at infinity upstream, to $(gH)^{\frac{1}{2}}$. In our discussion of slowly varying F, we only consider the case $\mathrm{d}F/\mathrm{d}t = O(\epsilon)$. A sudden wind flowing over a mountain ridge, tidal motions near coastal areas and underwater seismic disturbances are some of the applications of the model we consider here.

The shallow-water equations in the limit of no dispersion for $F = \text{const.} \neq 1$ were studied numerically by Houghton & Kasahara (1968). More recently, the behaviour of small-amplitude waves with $F = \text{const.}$ was discussed in a series of papers (Frenzen 1982; Cole 1983, 1985; Akylas 1984; Grimshaw & Smyth 1986; Mei 1986; Melville & Helfrich 1987; Smyth 1987; Wu 1987). The work in Frenzen (1982) is limited to the non-dispersive problem. That in Cole (1983) is limited to the case of steady flow, while the papers of Akylas (1984), Cole (1985) and Mei (1986) concern problems similar to ours. Melville & Helfrich (1987) assume a two-layer model and Grimshaw & Smyth (1986) consider a continuously stratified fluid. In all of these references, it is noted that the linearized theory breaks down for $F \approx 1$; the free surface height grows with time to eventually obey a Korteweg–de Vries (KdV)

equation with a forcing term depending on the given bottom disturbance. Frenzen (1982) only derives the non-dispersive limit for this equation. In Wu (1987), this forced KdV equation is derived, then solved numerically starting from a Boussinesq approximation and assuming unidirectional waves. The interesting feature of the mation and assuming unidirectional waves. The interesting feature of the solutions of the forced KdV equation is the periodic production of solitary waves which propagate essentially unchanged upstream. It therefore follows that for a certain range of parameters steady solutions do not exist for the transcritical flow problem (see Miles 1986).

Mathematically, the problem we have formulated is analogous to 'transient resonance' problems for systems of ordinary differential equations with prescribed slowly varying parameters as discussed by Kevorkian (1982, 1987). A closer connection exists with the problem of transition from supersonic to transonic flow in a stratified medium (see §5.3.4 of Kevorkian & Cole 1981). However, in the present case, as $F-1$ changes sign, the equations do not change type as they do when the Mach number passes slowly through unity. The common feature of all the above transient resonance problems is the breakdown of the basic asymptotic solution near the critical value of a given slowly varying parameter. This necessitates the introduction of an 'interior layer' expansion in the transcritical region, then matching this expansion with the precritical one in order to continue the solution. The essential effect of passage through the transcritical layer is the amplification of $O(\epsilon)$ disturbances to $O(\epsilon^{\frac{1}{2}})$ if $\mathrm{d}F/\mathrm{d}t = O(\epsilon)$.

We begin with the case $F = 0$, and introduce the Boussinesq approximation in which we keep track of the orders of magnitude of ignored terms. Thus, while this approximation provides a short-cut in comparison with the 'exact' formulation, it is only consistent to a limited order of accuracy which we establish in terms of ϵ, δ and ν and the interval in time over which uniformity is desired. We then reformulate our problem, give the Boussinesq approximation for arbitrary F, and express the governing equations in a coordinate system fixed to the bottom disturbance.

Section 3 gives a summary of results for the case $F = \text{const}$. If $F \neq 1$, the perturbations to the speed and free surface height are $O(\epsilon)$ so that the solution can be expressed in the form of a multiple-scale expansion involving x, t and the slow time $\tilde{t} = \epsilon t$. This expansion is derived to $O(\epsilon)$ and remains uniformly valid for $t = O(\epsilon^{-1})$. For the linearized problem it is well known (see Grimshaw & Smyth 1986) that the flow consists of three disturbances. This feature persists for the weakly nonlinear problem described by our multiple-scale expansion. The first disturbance is stationary over the bump and becomes singular (because of the presence of an $(F-1)$ divisor) as $F \to 1$. The two other disturbances, which we denote as 'f and g-waves', obey decoupled KdV equations. The f-waves evolve on the fast scale $\xi = x-(F+1)t$ and slow scale $\tilde{t}$ while the g-waves are functions of $\eta = x-(F-1)t$ and $\tilde{t}$.

In terms of the dimensionless variables that we have adopted, the solution for the f- and g-waves depends on the similarity parameter $\kappa \equiv \delta/\epsilon^{\frac{3}{2}}$. Thus, the asymptotic expansion of our solution is constructed in the limit $\epsilon \to 0, \delta \to 0$ with κ fixed. As discussed in Kevorkian & Cole (1981) and Frenzen & Kevorkian (1985), κ measures the relative importance of the dispersive and nonlinear effects and occurs as a multiplier of the third-derivative terms in each of the KdV equations for the f- and g-waves. If $\kappa = O(1)$, the cumulative effects of weak dispersion and weak nonlinearity are equally important. Dispersive effects produce 'ripples' in the solution and, in the absence of viscosity and surface tension, these ripples persist as $t \to \infty$. In the special

case $\kappa \equiv 0$ the weak nonlinear effects predominate over the weak dispersive effects. In this limiting case the *f*- and *g*-waves obey first-order quasi-linear equations which describe slowly varying non-dispersive waves which may steepen and break thus necessitating the introduction of bores. In our formulation $\kappa = (H/L)/(A/H)^{\frac{1}{2}}$ if $F \neq 1$. Therefore, setting $\kappa \equiv 0$ implies, in effect, that we assume $(H/L) \ll (A/H)^{\frac{1}{2}}$. In Grimshaw & Smyth (1986) a discussion is given of a 'hydraulic approximation' corresponding to $L \to \infty$ for a finite H. In a sense this is analogous to our limiting case $\kappa \equiv 0$.

We calculate the *f*- and *g*-waves by numerically integrating the corresponding KdV equations. These results are then substituted into the leading perturbation terms in our multiple-scale expansion to obtain a semianalytic solution to $O(\epsilon)$. This solution is significantly easier to calculate than an entirely numerical solution of the Boussinesq equations. Our numerical results highlight the importance of κ to the qualitative behaviour of the solution and provide a numerical assessment of the validity of the non-dispersive limit $\kappa \equiv 0$. If $\kappa \equiv 0$, the evolution equations are solved explicitly and exhibit the typical behaviour of steepening and eventual breaking of waves. In this regard, we derive the bore conditions which correspond to the integral conservation laws of mass and momentum. Our results are then compared to numerical integrations to verify the order of accuracy, the period of uniform validity, the time of breaking and the behaviour of solutions with bores.

An identical program is followed for the case $F = \text{const.} \approx 1$. It was shown by Yu (1988) that the condition that dictates the need for a different expansion as $F \to 1$ is that the similarity parameter $F^* \equiv |F-1|\epsilon^{-\frac{1}{2}}$ be $O(1)$. In this case the expansions must proceed in powers of $\epsilon^{\frac{1}{2}}$ and depend on a slow time $t^* = \epsilon^{\frac{1}{2}}t$. It also follows that the amplitude of perturbations for the speed and free surface height are $O(\epsilon^{\frac{1}{2}})$, therefore the appropriate similarity parameter which measures dispersive effects is now $\kappa^* = \delta/\epsilon^{\frac{1}{4}}$. The solution to $O(\epsilon^{\frac{1}{2}})$ can be expressed in terms of a single evolution equation which is a forced KdV equation in terms of t^* and x. This is the same as the result derived from two entirely different points of view by Cole (1985) and Wu (1987), and we confirm the numerical results concerning upstream-propagating solitary waves reported there. We also derive explicit analytic results for the non-dispersive limit and verify their accuracy with numerical integrations.

All the results presented in §3 are discussed in more detail in Yu (1988). These results provide the background for §4 where the problem of slow passage through the critical Froude number $F = 1$ is discussed. In this paper we assume that F is a given function of $\tilde{t}$ which equals unity at some $\tilde{t} = \tilde{t}_0$. Thus, a typical solution starts in a form similar to the one discussed in §3, then evolves slowly to become singular as $\tilde{t} \to \tilde{t}_0$. We construct a transcritical expansion for $\tilde{t} \approx \tilde{t}_0$ and match this with the precritical expansion. The matching determines the solution in the transcritical region completely and this solution is in turn matched with a third expansion valid for $\tilde{t} \gg \tilde{t}_0$. We show that the $O(\epsilon)$ initial perturbations amplify to become $O(\epsilon^{\frac{1}{2}})$ and these persist over an interval which lengthens slowly with time as F increases beyond the transcritical region. Again, our results are compared with numerical solutions in the various regions and are shown to be consistent.

2. Problem formulation, shallow-water approximation

2.1. *The exact problem*

We consider an 'ideal' fluid and ignore the effects of viscosity and surface tension, and also regard the density as a constant. As this 'exact' problem is irrotational, it

is conveniently defined in terms of a velocity potential which is expressed in dimensionless form as $\phi(\bar{x}, \bar{y}, \bar{t})$ and obeys (cf. equations (5.2.20)–(5.2.23) of Kevorkian & Cole 1981)

$$\delta^2\phi_{\bar{x}\bar{x}} + \phi_{\bar{y}\bar{y}} = 0; \quad \epsilon\bar{b} \leqslant \bar{y} \leqslant \epsilon\bar{b} + \bar{h}, \quad -\infty < \bar{x} < +\infty. \tag{2.1}$$

In a frame of reference where the flow has zero velocity at upstream infinity, the initial conditions are

$$\phi(\bar{x}, \bar{y}, 0^-) = 0; \quad \bar{h}(\bar{x}, 0^-) = 1 - \epsilon\bar{b}(\bar{x}, 0^-). \tag{2.2}$$

The imposed bottom disturbance $\bar{b}(\bar{x}, \bar{t})$ is in the form

$$\bar{b}(\bar{x}, \bar{t}) = \begin{cases} B(\bar{x} + t^+); & \bar{t} > 0, \\ B(\bar{x}); & \bar{t} < 0, \end{cases} \tag{2.3}$$

Here $B(x)$ is a prescribed isolated function, i.e. $B(s) = 0$ if $|s| > \frac{1}{2}$, and t^+ is the function of time defined by

$$t^+ = \int_0^{\bar{t}} F(\sigma\tau)\, \mathrm{d}\tau, \tag{2.4}$$

for a given function $F(\sigma\tau)$. This is the Froude number and the small parameter σ measures the slowness of variations of F on the $\bar{t}$-scale. The 'slow time' is $\tilde{t} = \sigma\bar{t}$, and in this paper we only study the case $\sigma = \epsilon$. The case $\sigma = \epsilon^2$ is also interesting and is analogous to the problem of very slow passage through resonance in ordinary differential equations (cf. §4 of Kevorkian 1982 and §5.3 of Kevorkian 1987).

The boundary conditions on the bottom and free surface are (cf. equations (5.2.21)–(5.2.23) of Kevorkian & Cole 1981)

$$\phi_{\bar{y}} = \epsilon\delta^2(\phi_{\bar{x}}\bar{b}_{\bar{x}} + \bar{b}_{\bar{t}}) \quad \text{on} \quad \bar{y} = \epsilon\bar{b}, \tag{2.5}$$

$$\phi_{\bar{t}} + \tfrac{1}{2}(\phi_{\bar{x}}^2 + \phi_{\bar{y}}^2/\delta^2) + \bar{h} + \epsilon\bar{b} - 1 = 0 \quad \text{on} \quad \bar{y} = \epsilon\bar{b} + \bar{h}, \tag{2.6}$$

$$\phi_{\bar{y}} = \delta^2[(\bar{h} + \epsilon\bar{b})_{\bar{t}} + \phi_{\bar{x}}(\bar{h} + \epsilon\bar{b})_{\bar{x}}] \quad \text{on} \quad \bar{y} = \epsilon\bar{b} + \bar{h}. \tag{2.7}$$

2.2. *The Boussinesq approximation*

An exact solution of (2.1)–(2.7) is out of reach because of the nonlinear boundary conditions, and one is led to seek solutions for the limiting case of small disturbances, $0 < \epsilon \ll 1$. A further approximation which still retains all the essential features of the nonlinear problem is provided by the 'shallow water' or 'long wave' limit $0 < \delta \ll 1$. The 'richest' approximation in this case has $\delta = O(\nu^{\frac{1}{2}})$, say $\delta = \kappa\nu^{\frac{1}{2}}$ as discussed in §5.2 of Kevorkian & Cole (1981) for the case of surface disturbances and a flat bottom. Frenzen & Kevorkian (1985) discuss the case of surface disturbances over a spatially slowly varying bottom.

For an arbitrary isolated bottom disturbance of order ϵ of the form (2.3) and (2.4), Yu (1988) shows that $\delta = O(\nu^{\frac{1}{2}}) = \kappa\nu^{\frac{1}{2}}$ is still the appropriate choice leading to the richest equations and that the Boussinesq approximation corresponding to (2.1)–(2.7) is now given by

$$\bar{h}_{\bar{t}} + (\bar{u}\bar{h})_{\bar{x}} = O(\nu^4), \tag{2.8a}$$

$$\bar{u}_{\bar{t}} + \bar{u}\bar{u}_{\bar{x}} + (\bar{h} + \epsilon\bar{b})_{\bar{x}} = -\tfrac{1}{3}\delta^2\bar{h}_{\bar{x}\bar{t}\bar{t}} - \tfrac{1}{2}\delta^2\epsilon\bar{b}_{\bar{x}\bar{t}\bar{t}} + O(\nu^3), \tag{2.8b}$$

with initial conditions

$$\bar{u}(\bar{x}, 0) = 0; \quad \bar{h}(\bar{x}, 0) = 1 - \epsilon\bar{b}(\bar{x}, 0), \tag{2.8c, d}$$

where $\bar{b}(\bar{x}, \bar{t})$ is prescribed in the form (2.3) and (2.4).

The solution of (2.8) corresponds to the solution of (2.1)–(2.7) in the following

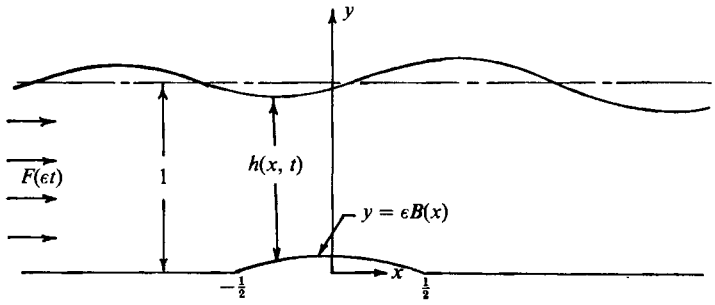

FIGURE 1. Geometry in the (x, y)-coordinate system attached to an isolated bump of fixed shape with a given $F(\epsilon t)$ at $x = -\infty$.

asymptotic sense: if we identify $\bar{h}$ in both cases and denote $\bar{u}$ as the average horizontal component of velocity, i.e.

$$\bar{u} = \frac{1}{\bar{h}} \int_{\epsilon\bar{b}}^{\epsilon\bar{b}+\bar{h}} \phi_{\bar{x}} \, \mathrm{d}\bar{y}, \tag{2.9}$$

then both problems have the same governing equations for the asymptotic expansions of $\bar{u}$ and $\bar{h}$ to the orders indicated by the error terms. In the non-dispersive limit $\kappa \equiv 0$, the bore conditions associated with (2.8*a*, *b*) are the same as those for a flat bottom, i.e.

$$\bar{C} = \frac{[\bar{u}\bar{h}]}{[\bar{h}]} = \frac{[\bar{u}^2\bar{h} + \frac{1}{2}\bar{h}^2]}{[\bar{u}\bar{h}]} \tag{2.10}$$

(see Stoker 1957). Here, $\bar{C}$ is the bore speed $\mathrm{d}\bar{x}/\mathrm{d}\bar{t}$, and $[\cdot]$ denotes the jump of a quantity across the bore.

In some applications, it is more convenient to study the solution in an (x, t)-coordinate system fixed to the isolated bump as shown in figure 1. The transformation relations are

$$x = \bar{x} + \int_0^t F(\epsilon\tau)\,\mathrm{d}\tau, \quad t = \bar{t}, \tag{2.11a}$$

$$\bar{u}(\bar{x}, \bar{t}) = u(x, t) - F(\epsilon t), \quad \bar{h}(\bar{x}, \bar{t}) = h(x, t), \tag{2.11b}$$

$$\bar{b}(\bar{x}, \bar{t}) = B(x), \tag{2.11c}$$

and the system (2.8) becomes

$$h_t + (uh)_x = O(\nu^4), \tag{2.12a}$$

$$u_t + uu_x + (h + \epsilon B)_x = \epsilon F_t - \tfrac{1}{3}\delta^2[F^2 h_{xxx} + 2Fh_{xxt} + h_{xtt}] - \delta^2\epsilon[\tfrac{1}{2}F^2 B_{xxx} + \tfrac{1}{3}F'h_{xx}] + O(\nu^3), \tag{2.12b}$$

$$u(x, 0) = F(0); \quad h(x, 0) = 1 - \epsilon B(x). \tag{2.12c}$$

Here F depends only on $\tilde{t}$, and B depends only on x.

3. Constant Froude number

3.1. *Non-critical case*, $F \neq 1$

As discussed in Kevorkian & Cole (1981), for the case $F = 0, \epsilon = 0$, the solution of (2.12) can be derived in the form of a multiple-scale expansion with respect to the small parameter ν and the two timescales t and $\tilde{t} = \nu t$.

We assume that $\nu = O(\epsilon)$, say $\nu = \epsilon$ for simplicity, and show that this leads to a consistent expansion as long as $F \neq 1$, i.e. the surface disturbances are of the same order as the prescribed bottom disturbance. We also set $\delta = \kappa\epsilon^{\frac{1}{2}}$ corresponding to the observation made in §2 that the richest equations result for $\delta = O(\nu^{\frac{1}{2}})$.

Thus, u and h are functions of x, t, the small parameter ϵ, and the two fixed parameters F and κ. We assume† that they have the following multiple-scale expansions:

$$u(x,t;\epsilon,F,\kappa) = F+\epsilon u_1(x,t,\tilde{t};F,\kappa)+\epsilon^2 u_2(x,t,\tilde{t};F,\kappa)+O(\epsilon^3), \tag{3.1a}$$

$$h(x,t;\epsilon,F,\kappa) = 1+\epsilon h_1(x,t,\tilde{t};F,\kappa)+\epsilon^2 h_2(x,t,\tilde{t};F,\kappa)+O(\epsilon^3), \tag{3.1b}$$

with $\tilde{t} = \epsilon t$.

The solution for u and h correct to $O(\epsilon)$ has the form

$$u(x,t;\epsilon,F,\kappa) = F+\epsilon\left\{-\frac{F}{F^2-1}B(x)+\tfrac{1}{2}f_1(\xi,\tilde{t};F,\kappa)-\tfrac{1}{2}g_1(\eta,\tilde{t};F,\kappa)\right\}+O(\epsilon^2), \tag{3.2a}$$

$$h(x,t;\epsilon,F,\kappa) = 1+\epsilon\left\{\frac{1}{F^2-1}B(x)+\tfrac{1}{2}f_1(\xi,\tilde{t};F,\kappa)+\tfrac{1}{2}g_1(\eta,\tilde{t};F,\kappa)\right\}+O(\epsilon^2), \tag{3.2b}$$

where ξ and η are the characteristic fast scales

$$\xi = x-(F+1)t; \quad \eta = x-(F-1)t. \tag{3.3}$$

Consistency conditions on the differential equations to $O(\epsilon^2)$ require that f_1 and g_1 satisfy the following KdV equations:

$$f_{1_{\tilde{t}}}+\tfrac{3}{4}f_1 f_{1_\xi}+\tfrac{1}{6}\kappa^2 f_{1_{\xi\xi\xi}} = 0; \quad g_{1_{\tilde{t}}}-\tfrac{3}{4}g_1 g_{1_\eta}-\tfrac{1}{6}\kappa^2 g_{1_{\eta\eta\eta}} = 0. \tag{3.4a, b}$$

These are the same evolution equations that one obtains for the case of surface disturbances over a flat bottom (see (5.2.82) of Kevorkian & Cole 1981). The initial conditions (2.12*c*) imply that

$$f_1(x,0;F,\kappa) = -\frac{FB(x)}{F+1}; \quad g_1(x,0;F,\kappa) = -\frac{FB(x)}{F-1}. \tag{3.5}$$

If F is not close to unity, the uncoupled evolution equations (3.4) subject to the initial conditions (3.5) define f_1 and g_1 uniquely. Once these functions have been derived, the solution for u and h correct to $O(\epsilon)$ is available from (3.2). Therefore, the solution to $O(\epsilon)$ consists of three non-interacting components – one that is stationary over the bump indicated by a constant times $B(x)$, a wave propagating to the right indicated by f_1, and a wave propagating to the right or left (depending upon $F > 1$ or $F < 1$) indicated by g_1. The singularity as $F \to 1$ is evident in the initial condition for g_1 and in the disturbance which remains stationary. This singularity implies that the assumed expansions (3.1) are not uniformly valid near $F = 1$. We shall discuss the solution for $F \approx 1$ in §3.2.

3.1.1. *The non-dispersive problem*

For $\kappa \equiv 0$, the solution to the corresponding evolution equations (3.4) has the compact form

$$f_1 = -\frac{F}{F+1}B(\xi_0); \quad g_1 = -\frac{F}{F-1}B(\eta_0), \tag{3.6a, b}$$

† Actually, the u_i and h_i in (3.1) should also depend on the slower scales $\epsilon^2 t, \epsilon^3 t$, etc. However, as we are only interested in results accurate to $O(\epsilon)$, the dependence of the solution on $\epsilon^2 t, \ldots$ is not pertinent; to determine this dependence in u_1 and h_1, for example, one would have to consider the $O(\epsilon^3)$ terms in (2.8).

where ξ_0 and η_0 are constants along the respective characteristics, defined implicitly by

$$\xi_0-\xi-\frac{3F}{4(F+1)}B(\xi_0)\tilde{t}=0; \quad \eta_0-\eta+\frac{3F}{4(F-1)}B(\eta_0)\tilde{t}=0. \tag{3.6c, d}$$

The solution of (3.6) is unique as long as neither of the two families (3.6*c*) and (3.6*d*) has an envelope. The details of how to fit a bore when characteristics intersect are similar to those discussed in §5.1.2 of Kevorkian & Cole (1981) for the analogous problem in acoustics. In the present case the exact bore conditions (2.10) imply the following conditions for $\mathrm{d}\xi/\mathrm{d}\tilde{t}$ and $\mathrm{d}\eta/\mathrm{d}\tilde{t}$:

$$\frac{\mathrm{d}\xi}{\mathrm{d}\tilde{t}}=\tfrac{3}{8}(f_1^+ + f_1^-); \quad \frac{\mathrm{d}\eta}{\mathrm{d}\tilde{t}}=-\tfrac{3}{8}(g_1^+ + g_1^-), \tag{3.7a, b}$$

where the $\pm$ superscripts indicate values on either side of a bore. Therefore the two physically consistent divergence forms of the evolution equations for f_1 and g_1 are

$$(f_1)_{\tilde{t}}+(\tfrac{3}{8}f_1^2)_{\xi}=0; \quad (g_1)_{\tilde{t}}-(\tfrac{3}{8}g_1^2)_{\eta}=0. \tag{3.8a, b}$$

Although (3.7) gives the two bore speeds to $O(\epsilon)$, bore trajectories in the (x,t)-plane are only defined to $O(1)$ for large time t (see Yu 1988).

For the disturbance due to the parabolic bump

$$B(x)=\begin{cases}(1-4x^2), & |x|\leqslant\tfrac{1}{2},\\ 0, & |x|>\tfrac{1}{2},\end{cases} \tag{3.9}$$

we compute

$$f_1=-\frac{F(1-4\xi_0^2)}{F+1}, \tag{3.10}$$

where

$$\xi_0-\xi-\frac{3F\tilde{t}}{4(F+1)}(1-4\xi_0^2)=0. \tag{3.11}$$

Thus, the initial value of f_1 propagates unchanged along the straight characteristics defined by (3.11). To express f_1 as a function of ξ and $\tilde{t}$, we solve the quadratic (3.11) for ξ_0 and use the root (the other root is spurious)

$$\xi_0=\frac{-1+[1+16c\tilde{t}(\xi+c\tilde{t})]^{\frac{1}{2}}}{8c\tilde{t}}, \tag{3.12a}$$

where we have introduced the notation

$$c=3F/4(F+1). \tag{3.12b}$$

Using (3.12*a*) in (3.10) defines f_1 in the $(\xi,\tilde{t})$-plane:

$$f_1(\xi,\tilde{t};F,0)=\frac{1+8\xi c\tilde{t}-[1+16c\tilde{t}(\xi+c\tilde{t})]^{\frac{1}{2}}}{6c\tilde{t}^2}. \tag{3.13}$$

The solution is unique as long as

$$0\leqslant\tilde{t}\leqslant\tilde{t}_0\equiv\tfrac{1}{4}c=\frac{F+1}{3F}. \tag{3.14}$$

The results for the g_1 wave can be derived from the above by noting that the two problems are equivalent under the transformation $\xi_0\to-\eta_0, \xi\to-\eta, \tilde{t}\to\tilde{t}, c\to d$, where d is the constant

$$d=\frac{3F}{4(F-1)}. \tag{3.15}$$

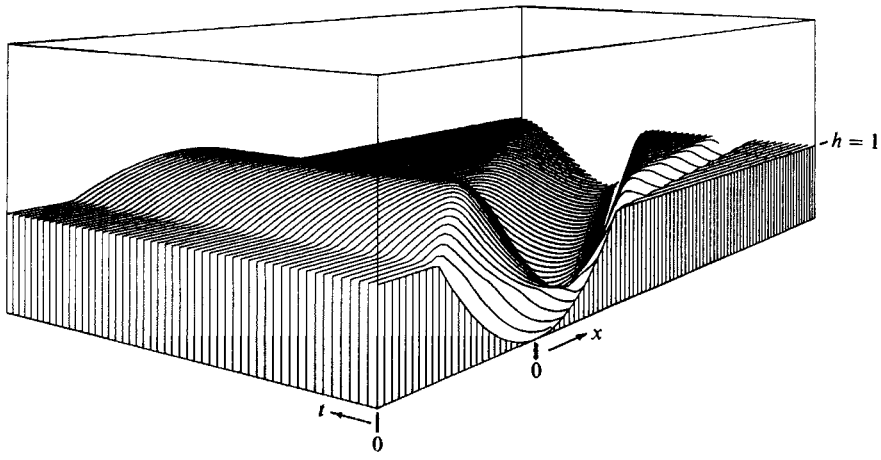

FIGURE 2. Evolution of the free surface for short times with $F = 2, \epsilon = 0.1$.

3.1.2. *Numerical solutions, discussion of results*

We first verify the accuracy of the asymptotic results for the non-dispersive case ($\kappa \equiv 0$) by numerically solving the exact problem. We rescale the characteristic variables and solve the equations by an explicit finite-difference method (see Yu 1988). The case $F = 2, \epsilon = 0.1$ provides a stringent test of the asymptotic validity of the theory for times up to about $t = 10$, which is certainly $O(\epsilon^{-1})$. According to (3.14) the f_1 wave breaks at $t = 5$ and the g_1 wave breaks at $t = \frac{5}{3}$. Both of these breaking times are in the interval of our numerical results, and we are able to compare solutions with well-developed bores.

Figure 2 gives a perspective view of the short-term evolution of h with time. The x- and t-axes are measured along the base of the diagram, and the various curves drawn at each time represent $h-1$. In figure 3, we show the numerical (solid curve) and theoretical (dashed curve) values of h as contributed by the f_1 and g_1 waves at $t = 10$; the stationary disturbance over the bump is not shown. The location of the bore for the f_1 wave is indeed accurately predicted, and so are the values of h. The maximum error for all points away from the bore is 0.7×10^{-2} while the maximum error near the bore is 1.25×10^{-2}. As for the g_1 wave, the maximum error in h away from the bore is still less than 10^{-2}, while near the bore it is 8×10^{-2}, and this is entirely due to the error in the bore location. In fact, the time elapsed from the formation of the bore for the g_1 wave is $8.3 = 0.83\epsilon^{-1}$ and may be regarded as $O(\epsilon^{-1})$. As mentioned earlier, our results only predict the bore location for times of order unity from the time of the bore formation, and the above accuracy is therefore consistent.

For the dispersive case $\kappa \neq 0$, we numerically integrate the two evolution equations (3.4) and use the results in (3.2) to compute u and h. The key statement of the numerical algorithm is

$$f_j^{n+1} = f_j^n - \tfrac{3}{4}\Delta t f_j^n \frac{f_{j+1}^n - f_{j-1}^{n+1}}{2\Delta x} - \tfrac{1}{6}\kappa^2 \Delta t \frac{f_{j+3}^n - 3f_{j+1}^n + 3f_{j-1}^{n+1} - f_{j-3}^{n+1}}{(2\Delta x)^3}. \tag{3.16}$$

This method is always stable. For the method given in Copeland (1977), the time step Δt is very restrictive ($\Delta t \sim (\Delta x)^3$). If the condition $\Delta t \leqslant 2.4(\Delta x)^3/\kappa^2$ is satisfied, the algorithm (3.16) is consistent.

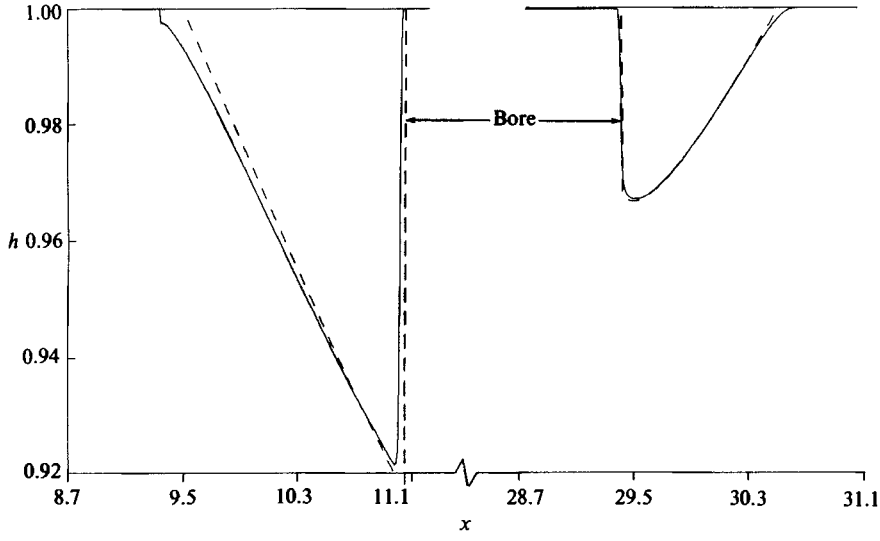

FIGURE 3. Free surface at a large time ($t = 10$) for $F = 2, \epsilon = 0.1$. The solid curve shows the numerical result.

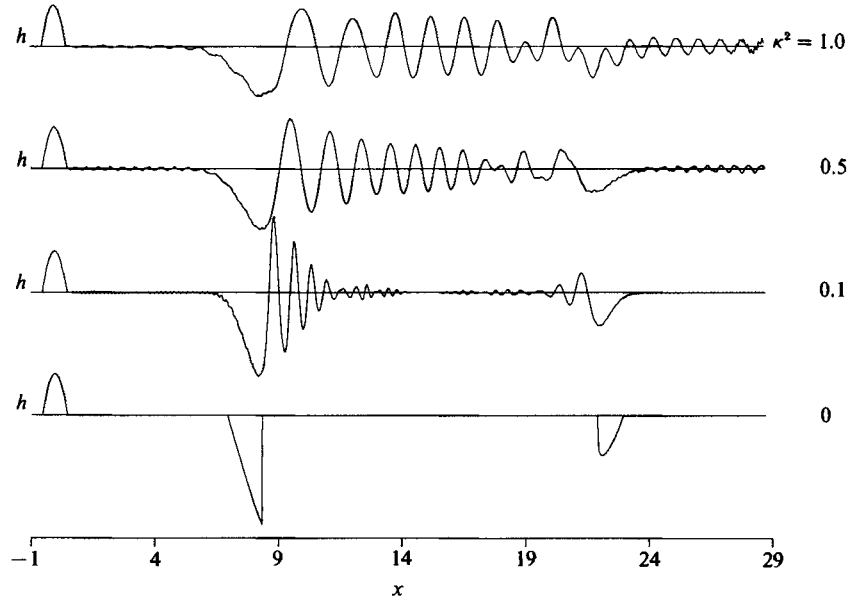

FIGURE 4. Free surface at $t = 7.5, F = 2, \epsilon = 0.1$ for various κ^2.

The role of the dispersive term in (3.4) is shown in figure 4, where we have calculated h as a function of x at $t = 7.5, F = 2$ and the four values of $\kappa^2 = 0, 0.1, 0.5, 1.0$. For $\kappa^2 = 0$, we have the three isolated disturbances already seen in figure 2. As κ^2 increases, ripples of increasing amplitude develop, primarily in the interval between the f_1 and g_1 waves. The three main disturbances are easy to identify for $\kappa^2 = 0.1$ and even for $\kappa^2 = 0.5$. However, for $\kappa^2 = 1.0$, the ripples have roughly the same amplitude as the f_1, g_1 waves, and only the disturbance over the bump can be

distinguished separately. As is evident from figure 4, it is not reasonable to ignore the dispersive terms if κ^2 is any larger than 0.1.

Of course, one has to also take viscous effects into account in a physically realistic model. In a model with no dissipation such as ours *the dispersive solutions need not tend to the non-dispersive ones as* $\kappa^2 \to 0$ (see also the discussion at the end of §3.2). In fact the question of what happens as $\kappa^2 \to 0$ is only meaningful in a setting including dissipation. This question is discussed in §13.15 of Whitham (1974) for a mathematical model of the KdV equation with an added second-derivative term to simulate viscous effects. A systematic treatment of viscous effects in the actual physical problem of water waves is very difficult. However, based on the linear theory (e.g. see Mainardi & LeBlond 1987 and the references cited there), one expects viscosity to attenuate the amplitude of disturbances and to suppress the ripples introduced by dispersion. Therefore, in a sense, dispersion and viscous effects tend to cancel, and the dominant flow behaviour is expected to be governed at least qualitatively by the present model with $\kappa^2 = 0$.

3.2. *Critical case,* $F \approx 1$

It was pointed out in §3.1 that the multiple-scale expansion (3.2) breaks down for $F \approx 1$. The basic reason for the non-uniformity can be traced to the contradictory implicit assumptions (when $F \approx 1$) that: (i) surface disturbances are $O(\epsilon)$ and (ii) that disturbances propagate with near characteristic speeds $F+1$ and $F-1$. When $F \approx 1$ one of the characteristic speeds is very small, i.e. the associated disturbance remains stationary over the bump. This in turn implies that perturbations over the bump grow with time, in contradiction to the assumed order of magnitude of the free surface perturbation.

An order of magnitude analysis shows that the following rescalings are appropriate for $F \approx 1$ (see Yu 1988):

$$F-1 = \epsilon^{\frac{1}{2}}F^*; \quad \nu = \epsilon^{\frac{1}{2}}; \quad \delta = \epsilon^{\frac{1}{4}}\kappa^*; \quad t^* = \epsilon^{\frac{1}{2}}t. \tag{3.17}$$

The multiple-scale expansions for u and h then take the form (cf. (3.1))

$$u = 1+\epsilon^{\frac{1}{2}}[F^*+u_1^*(x,t,t^*;F^*,\kappa^*)]+\epsilon u_2^*(x,t,t^*;F^*,\kappa^*)+O(\epsilon^{\frac{3}{2}}) \tag{3.18a}$$

$$h = 1+\epsilon^{\frac{1}{2}}h_1^*(x,t,t^*;F^*,\kappa^*)+\epsilon h_2^*(x,t,t^*;F^*,\kappa^*)+O(\epsilon^{\frac{3}{2}}). \tag{3.18b}$$

We find that u and h depend only on g_1^* to $O(\epsilon^{\frac{1}{2}})$ and are given by

$$u(x,t;\epsilon,F,\kappa) = 1+\epsilon^{\frac{1}{2}}[F^*-\tfrac{1}{2}g_1^*(x,t^*;F^*,\kappa^*)]+O(\epsilon), \tag{3.19a}$$

$$h(x,t;\epsilon,F,\kappa) = 1+\tfrac{1}{2}\epsilon^{\frac{1}{2}}g_1^*(x,t^*;F^*,\kappa^*)+O(\epsilon). \tag{3.19b}$$

Here g_1^* satisfies the evolution equation

$$g_{1_{t^*}}^*+(F^*-\tfrac{3}{4}g_1^*)g_{1_x}^*-\tfrac{1}{6}\kappa^{*2}g_{1_{xxx}}^* = B_x, \tag{3.20}$$

with initial condition

$$g_1^*(x,0;F^*,\kappa^*) = 0. \tag{3.21}$$

It is shown in Cole (1985) that, even for the case of deep water ($\delta = 1$), the appropriate evolution equation if $F \approx 1$ is the forced KdV equation (3.20) which is solved numerically there for the special case of a delta-function bump. This equation is also derived in Wu (1987) then solved numerically starting from the Boussinesq approximation and assuming unidirectional flow. In the remainder of this section we give a summary of results which parallel those in Grimshaw & Smyth (1986).

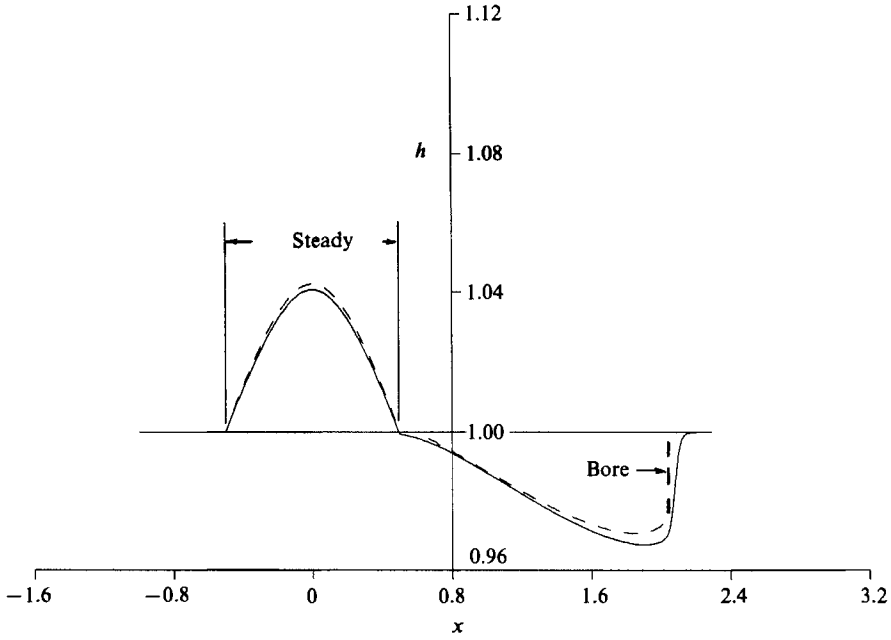

FIGURE 5. Free surface at $t^* = 1$ for $\kappa^* = 0, \epsilon = 0.01, F^* = 1.5 > (3/2)^{\frac{1}{2}}$. Steady solution over the bump. The solid curve shows the numerical result.

(i) The non-dispersive problem. If $\kappa^* = 0$, the problem can be expressed in the compact form

$$w_{t^*} + ww_x = -\tfrac{3}{4}B_x; \quad w(x, 0; F^*) = F^*, \tag{3.22a, b}$$

through the new variable

$$w(x, t^*; F^*) \equiv F^* - \tfrac{3}{4}g_1^*(x, t^*; F^*, 0). \tag{3.23}$$

The physically consistent divergence form and associated bore condition for this equation are

$$w_{t^*} + (\tfrac{1}{2}w^2)_x = -\tfrac{3}{4}B_x; \quad \frac{\mathrm{d}x}{\mathrm{d}t^*} = \tfrac{1}{2}(w^+ + w^-). \tag{3.24}$$

A complete explicit solution for the case $\kappa^* = 0, B(x) = 1 - 4x^2$ can be found in Yu (1988). Representative charcteristic curves shown there are in qualitive agreement with the numerically calculated curves given in figure 2 of Grimshaw & Smyth (1986). The nature of the solution depends on whether $F^* \gtrless (3/2)^{\frac{1}{2}}$ as shown in figures 5 and 6 corresponding to $F^* = 1.5 > (3/2)^{\frac{1}{2}}$ and $F^* = 1.15 < (3/2)^{\frac{1}{2}}$ respectively. In particular, a stationary solution over the bump is possible only if $F^* > (3/2)^{\frac{1}{2}}$.

(ii) Numerical Results. The solid curves in figures 5 and 6 show the numerical solution of the exact non-dispersive equations. The error in both cases is of order $\epsilon = 0.01$ at the time $t = 10 = O(\epsilon^{-\frac{1}{2}})$, as expected from the order of accuracy of the theory.

We use the same algorithm (3.16) as in §3.1.2 to solve the forced KdV equation (3.20) for g_1^*. The results for $h = 1 + \epsilon^{\frac{1}{2}}g_1^*$ are shown in figure 7 calculated for the times $t^* = 6$, 12, 18, 24 and the case $\kappa^* = 1, F^* = 0$. These are in qualitative agreement with the numerical results calculated for a delta-function bump in Cole (1985) for the case of $\delta = 1$. Our results also agree with the numerical solutions given in Wu (1987). One observes the periodic production of solitary waves which propagate essentially

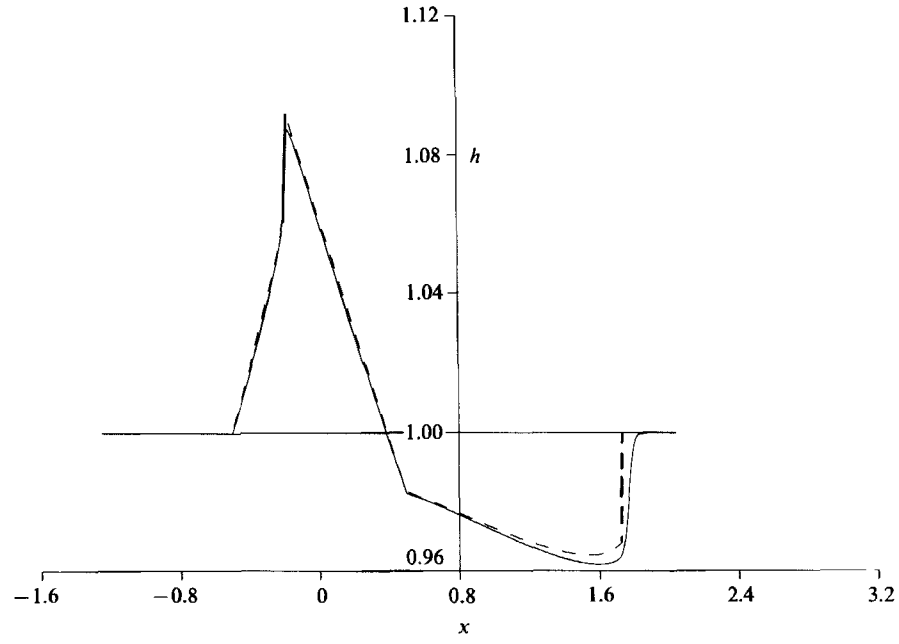

FIGURE 6. Free surface at $t^* = 1$ for $\kappa^* = 0, \epsilon = 0.01, F^* = 1.15 < (3/2)^{\frac{1}{2}}$. No steady solution over the bump. The solid curve shows the numerical result.

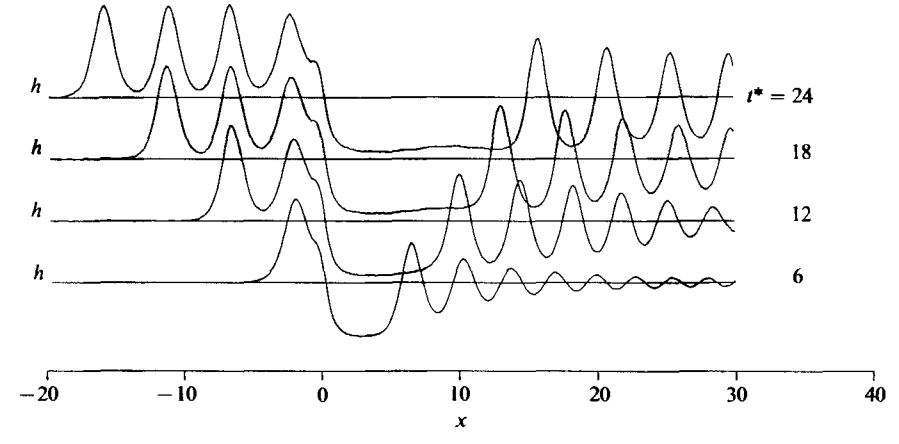

FIGURE 7. Free surface at various t^* for $\kappa^* = 1, \epsilon = 0.01, F^* = 0$.

unchanged upstream. There is a region of $h < 1$ just downstream of the bump which grows in width as time increases. Just downstream of this region we see large-amplitude nonlinear waves which gradually decay in amplitude further downstream and tend to become linear. A further study shows that these large-amplitude waves are in fact solitary waves with different bases and they propagate downstream as if there were no other waves around. The starting time for the generation of solitary waves increases as F^* increases and so does the production period of these solitary waves.

To conclude this discussion, we illustrate in figure 8 the role of κ^* in the solution for the conditions used to calculate figure 6, i.e. $F = 1.115, \epsilon = 0.01, t = 10$

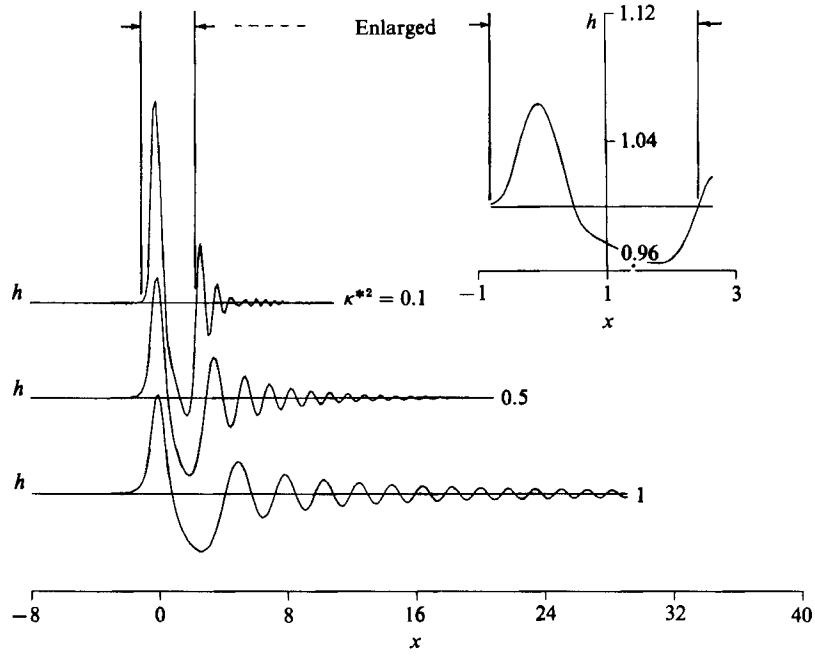

FIGURE 8. Free surface at $t^* = 1, \epsilon = 0.01, F^* = 1.15$ for various κ^{*2}. Compare enlarged view with solution for $\kappa^* = 0$ given in figure 6.

($F^* = 1.15, t^* = 1.0$). If $\kappa^* = 1.0$, the solution downstream of the bump has a significant oscillatory behaviour which is absent in the limiting case $\kappa^* = 0$ given in figure 6. As κ^* decreases, the amplitude and wavelength of oscillations decrease. Note the close correspondence between the surface profile shown in figure 6 and the enlarged view of the solution over the bump for $\kappa^{*2} = 0.1$. For this value of κ^*, the dispersive effects are negligible everywhere except just upstream and just downstream of the bump. However, the limiting solution of the dispersive problem as $\kappa^2 \to 0$ is seen to differ significantly from the non-dispersive result in the vicinity of the two bores. Again, a systematic treatment must also include the effects of dissipation.

4. Variable Froude number, $F(\tilde{t})$

In this section we consider flows with a prescribed $F(\tilde{t})$ over an interval in $\tilde{t}$ which contains the critical time $\tilde{t}_0$ at which $F(\tilde{t}_0) = 1$. Now, a single expansion cannot define the solution for all $\tilde{t}$ and we construct and match three different expansions, one valid in the precritical region $\epsilon^{\frac{1}{3}} \ll (\tilde{t}_0 - \tilde{t})$, the second valid in the transcritical region $(\tilde{t} - \tilde{t}_0) = O(\epsilon^{\frac{1}{3}})$, and the third valid in the postcritical region $\epsilon^{\frac{1}{3}} \ll (\tilde{t} - \tilde{t}_0)$. This situation is analogous to that of 'transient resonance' for systems of ordinary differential equations as discussed in Kevorkian (1987). It is also quite similar to the problem of transition from supersonic to transonic flow as discussed in §5.3.4 of Kevorkian & Cole (1981).

4.1. *Precritical expansion*, $\epsilon^{\frac{1}{3}} \ll (\tilde{t}_0 - \tilde{t})$

It is more convenient to calculate the solution in terms of the coordinate system for (2.8) in which the bump moves with speed $F(\tilde{t})$. Thus, we wish to solve the initial-value problem (2.8) with $\bar{b} = B(\bar{x} + t^+)$ as defined in (2.3) and (2.4).

We expand $\bar{u}$ and $\bar{h}$ in the multiple-scale form:

$$\bar{u}(\bar{x},\bar{t};\epsilon,\kappa) = \epsilon\bar{u}_1(\bar{x},\bar{t},\tilde{t};\kappa)+\epsilon^2\bar{u}_2(\bar{x},\bar{t},\tilde{t};\kappa)+O(\epsilon^3), \tag{4.1a}$$

$$\bar{h}(\bar{x},\bar{t};\epsilon,\kappa) = 1+\epsilon\bar{h}_1(\bar{x},\bar{t},\tilde{t};\kappa)+\epsilon^2\bar{h}_2(\bar{x},\bar{t},\tilde{t};\kappa)+O(\epsilon^3), \tag{4.1b}$$

where $\tilde{t} = \epsilon\bar{t} = \epsilon t$, and find that $\bar{u}_1$ and $\bar{h}_1$ have the form (cf. (3.2))

$$\bar{u}_1 = -\frac{F(\tilde{t})\,B(\bar{x}+t^+)}{F^2(\tilde{t})-1}+\tfrac{1}{2}\bar{f}_1(\bar{\xi},\tilde{t};\kappa)-\tfrac{1}{2}\bar{g}_1(\bar{\eta},\tilde{t};\kappa), \tag{4.2a}$$

$$\bar{h}_1 = \frac{B(\bar{x}+t^+)}{F^2(\tilde{t})-1}+\tfrac{1}{2}\bar{f}_1(\bar{\xi},\tilde{t};\kappa)+\tfrac{1}{2}\bar{g}_1(\bar{\eta},\tilde{t};\kappa), \tag{4.2b}$$

where

$$\bar{\xi} = \bar{x}-\bar{t}; \quad \bar{\eta} = \bar{x}+\bar{t}. \tag{4.3a, b}$$

The singularity at $\tilde{t} = \tilde{t}_0$ (where $F(\tilde{t}_0) = 1$) is exhibited by the first term on the right-hand sides of (4.2). Here, in contrast to the case $F = \text{const.} \approx 1$, the solution is initially well behaved; it only becomes singular as $\tilde{t}\to\tilde{t}_0$. Actually, the matching of solutions to be discussed in §4.2 shows that (4.2) is valid for $(\tilde{t}_0-\tilde{t}) \gg \epsilon^{\frac{1}{2}}$; this expansion only becomes singular for $(\tilde{t}-\tilde{t}_0) = O(\epsilon^{\frac{1}{3}})$. It will also be shown in §4.2 that the singular terms in $\bar{u}_1$ and $\bar{h}_1$ match with corresponding terms in the transcritical solution.

Consistency requirements on the solution to $O(\epsilon^2)$ provide the evolution equations for $\bar{f}_1$ and $\bar{g}_1$ in a form identical to (3.4), i.e.

$$\bar{f}_{1_{\tilde{t}}}+\tfrac{3}{4}\bar{f}_1\bar{f}_{1_{\bar{\xi}}}+\tfrac{1}{6}\kappa^2\bar{f}_{1_{\bar{\xi}\bar{\xi}\bar{\xi}}} = 0; \quad \bar{g}_{1_{\tilde{t}}}-\tfrac{3}{4}\bar{g}_1\bar{g}_{1_{\bar{\eta}}}-\tfrac{1}{6}\kappa^2\bar{g}_{1_{\bar{\eta}\bar{\eta}\bar{\eta}}} = 0. \tag{4.4a, b}$$

These are to be solved numerically for the initial conditions,

$$\bar{f}_1(\bar{x},0;\kappa) = -\frac{F(0)}{F(0)+1}B(\bar{x}); \quad g_1(\bar{x},0;\kappa) = -\frac{F(0)}{F(0)-1}B(\bar{x}), \tag{4.5a, b}$$

that result when (4.2) is substituted into (2.8c, d).

For the non-dispersive limit $\kappa \equiv 0$, we can solve (4.4) explicitly and find

$$\bar{f}_1(\bar{\xi},\tilde{t};\kappa) = -\frac{F(0)}{F(0)+1}B(\bar{\xi}^*); \quad \bar{g}_1(\bar{\eta},\tilde{t};\kappa) = -\frac{F(0)}{F(0)-1}B(\bar{\eta}^*), \tag{4.6a, b}$$

where $\bar{\xi}^* = \text{const.}$ and $\bar{\eta}^* = \text{const.}$ are the characteristic curves defined in the implicit form (cf. (3.6)):

$$\bar{\xi}^* = \bar{x}-\bar{t}+\tfrac{3}{4}\frac{F(0)\,B(\bar{\xi}^*)}{F(0)+1}\tilde{t}; \quad \bar{\eta}^* = \bar{x}+\bar{t}-\tfrac{3}{4}\frac{F(0)\,B(\bar{\eta}^*)}{F(0)-1}\tilde{t}. \tag{4.7a, b}$$

In the coordinate system (2.11) attached to the bump, we have

$$u(x,t;\epsilon,0) = F(\tilde{t})+\epsilon\left\{-\frac{F(\tilde{t})\,B(x)}{F^2(\tilde{t})-1}-\frac{F(0)\,B(\bar{\xi}^*)}{2[F(0)+1]}+\frac{F(0)\,B(\bar{\eta}^*)}{2[F(0)-1]}\right\}+O(\epsilon^2), \tag{4.8a}$$

$$h(x,t;\epsilon,0) = 1+\epsilon\left\{\frac{B(x)}{F^2(\tilde{t})-1}-\frac{F(0)\,B(\bar{\xi}^*)}{2[F(0)+1]}-\frac{F(0)\,B(\bar{\eta}^*)}{2[F(0)-1]}\right\}+O(\epsilon^2), \tag{4.8b}$$

where the characteristic curves are now defined by

$$\bar{\xi}^* = x-\int_0^t F(\epsilon\tau)\,\mathrm{d}\tau-t+\tfrac{3}{4}\frac{F(0)\,B(\bar{\xi}^*)}{F(0)+1}\tilde{t}, \tag{4.9a}$$

$$\bar{\eta}^* = x-\int_0^t F(\epsilon\tau)\,\mathrm{d}\tau+t-\tfrac{3}{4}\frac{F(0)\,B(\bar{\eta}^*)}{F(0)-1}\tilde{t}. \tag{4.9b}$$

For the purposes of matching the above solution with the one valid in the transcritical region, we note that the characteristic variables, S_1 and R_1 are given by

$$S_1(x,t,\tilde{t};0) \equiv h_1+u_1 = -\frac{B(x)}{F(\tilde{t})+1}-\frac{F(0)B(\bar{\xi}^*)}{F(0)+1}, \tag{4.10a}$$

$$R_1(x,t,\tilde{t};0) \equiv h_1-u_1 = \frac{B(x)}{F(\tilde{t})-1}-\frac{F(0)B(\bar{\eta}^*)}{F(0)-1}. \tag{4.10b}$$

4.2. *Transcritical solution,* $|\tilde{t}-\tilde{t}_0| = O(\epsilon^{\frac{1}{2}})$; *matching*

Based on the order of magnitude analysis for the case F = const., we conclude that δ and $\tilde{t}$ must be rescaled as follows:

$$\delta = \epsilon^{\frac{1}{4}}\kappa^*; \quad t^* = \frac{1}{\epsilon^{\frac{1}{2}}}[(\tilde{t}-\tilde{t}_0)+\beta_1(\tilde{t}-\tilde{t}_0)^2], \tag{4.11a, b}$$

where β_1 is to be determined by matching the characteristics of the precritical and transcritical solutions.

Assuming that $F(\tilde{t})$ is analytic near $\tilde{t}=\tilde{t}_0$ and that $F-1$ has a simple zero there, we have the expansion

$$F(\tilde{t}) = 1+a_1(\tilde{t}-\tilde{t}_0)+a_2(\tilde{t}-\tilde{t}_0)^2+O((\tilde{t}-\tilde{t}_0)^3), \tag{4.12}$$

with known constants $a_1 \neq 0$ and a_2. Expressing $F(\tilde{t})$ in terms of t^* gives

$$F(\tilde{t}) = 1+a_1 t^*\epsilon^{\frac{1}{2}}+O(\epsilon). \tag{4.13}$$

In view of (4.13), we seek a solution in the following multiple-scale form (cf. (3.19)):

$$u(x,t;\epsilon,\kappa) = 1+\epsilon^{\frac{1}{4}}[a_1 t^*+u_1^*(x,t,t^*;\kappa^*)]+\epsilon u_2^*(x,t,t^*;\kappa^*)+O(\epsilon^{\frac{3}{4}}), \tag{4.14a}$$

$$h(x,t;\epsilon,\kappa) = 1+\epsilon^{\frac{1}{4}}h_1^*(x,t,t^*;\kappa^*)+\epsilon h_2^*(x,t,t^*;\kappa^*)+O(\epsilon^{\frac{3}{4}}), \tag{4.14b}$$

where $\kappa^* = \epsilon^{\frac{1}{4}}\kappa$. We find that u_1^* and h_1^* have the form

$$u_1^* = \tfrac{1}{2}f_1^*(\zeta,t^*;\kappa^*)-\tfrac{1}{2}g_1^*(x,t^*;\kappa^*), \tag{4.15a}$$

$$h_1^* = \tfrac{1}{2}f_1^*(\zeta,t^*;\kappa^*)+\tfrac{1}{2}g_1^*(x,t^*;\kappa^*), \tag{4.15b}$$

where $\zeta = x-2t$. Consistency of the solution to $O(\epsilon)$ then requires that f_1^* and g_1^* satisfy the following variable-coefficient KdV equations:

$$f_{1_{t^*}}^*+(a_1 t^*+\tfrac{3}{4}f_1^*)f_{1_\zeta}^*+\tfrac{1}{6}\kappa^{*2}f_{1_{\zeta\zeta\zeta}}^* = 0, \tag{4.16a}$$

$$g_{1_{t^*}}^*+(a_1 t^*-\tfrac{3}{4}g_1^*)g_{1_x}^*-\tfrac{1}{6}\kappa^{*2}g_{1_{xxx}}^* = B_x. \tag{4.16b}$$

Changing the dependent variable in (4.16*b*) according to

$$w = a_1 t^*-\tfrac{3}{4}g_1^*, \tag{4.17}$$

gives the forced KdV equation

$$w_{t^*}+ww_x-\tfrac{1}{6}\kappa^{*2}w_{xxx} = a_1-\tfrac{3}{4}B_x, \tag{4.18}$$

and a similar result follows for f_1^*.

One must keep in mind that now the solution of (4.18) is only valid for a short period of order $\epsilon^{\frac{1}{2}}$ in $\tilde{t}$ near $\tilde{t}_0$ (or for a period of order $\epsilon^{-\frac{1}{2}}$ in t). One of the interesting features discussed in §3.2 for the solution of the forced KdV equation (3.20) is the periodic generation of upstream-travelling solitary waves at a rate which is $O(1)$ in t^*. In the present case, this train of solitary waves will not have time to fully develop

if a_1 is not small because the transcritical solution only lasts for a period of order unity in t^*.

A complete description of the flow as F evolves from its initial value through $F = 1$ requires the matching of the two solutions of (4.4) and (4.18). A systematic matching requires that one be able to derive the asymptotic behaviour of the precritical solution as $\tilde{t} \to \tilde{t}_0$, and the asymptotic behaviour of the transcritical solution as $t^* \to -\infty$. The case where $\kappa^* \neq 0$ is discussed with a specific example in §5.4 of Yu (1988). Here we concentrate on the non-dispersive problem $\kappa^* \equiv 0$ for which explicit results can be derived.

The solution of (4.16) for $\kappa^* \equiv 0$ has the form

$$f_1^*(\zeta, t^*; 0) = \Phi^*(\zeta - \tfrac{3}{4} f_1^* t^* - \tfrac{1}{2} a_1 t^{*2}), \tag{4.19a}$$

$$g_1^*(x, t^*; 0) = \tfrac{4}{3}[a_1 t^* - w(x, t^*)], \tag{4.19b}$$

where the definition of w depends on x (cf. (4.18) and (3.9)). For $|x| \leqslant \frac{1}{2}$ we have

$$w^2 = c_1 + 2a_1 x - \tfrac{3}{2}(1 - 4x^2); \quad c_1 = \text{const.}, \tag{4.20a}$$

on the characteristic curves defined implicitly by

$$\left(x + \tfrac{1}{6} a_1 + \frac{w}{\sqrt{6}}\right) e^{-\sqrt{6} t^*} = c_2; \quad c_2 = \text{const.} \tag{4.20b}$$

If $|x| > \frac{1}{2}$, we have

$$w = a_1 t^* + c_3 \quad \text{on} \quad w^2 = 2a_1 x + c_4; \quad c_3, c_4 = \text{const.} \tag{4.21a, b}$$

In contrast to the case $F = \text{const.}$, where the integration constants were defined by the initial conditions, we must now match the transcritical and precritical solutions in order to determine $c_1, \ldots, c_4$, and this is discussed next.

Again it is useful to express the results in terms of the characteristic variables $S_1^* \equiv h_1^* + u_1^*$ and $R_1^* \equiv h_1^* - u_1^*$, and in this case we simply have

$$S_1^*(x, t, t^*; 0) = f_1^*; \quad R_1^*(x, t, t^*; 0) = g_1^*. \tag{4.22a, b}$$

As the transcritical solution has not been determined beyond $O(\epsilon^{\frac{1}{3}})$, we can only match to this order. This consists of matching ϵS_1 as given by (4.10a) with $\epsilon^{\frac{1}{3}} S_1^*$ to $O(\epsilon^{\frac{1}{3}})$ along the characteristics which correspond to $\bar{\xi}^* = \text{const.}$ in the precritical region. Also, we must match ϵR_1 as given by (4.10b) with $\epsilon^{\frac{1}{3}} R_1^*$ along the characteristics which correspond to $\bar{\eta}^* = \text{const.}$

We follow the procedure discussed in Kevorkian & Cole (1981) and introduce the matching variable t_α defined by

$$t_\alpha = \frac{\tilde{t} - \tilde{t}_0}{\epsilon^\alpha}, \tag{4.23}$$

where α is a constant in some overlap domain $0 \leqslant \alpha_1 < \alpha < \alpha_2 \leqslant \frac{1}{2}$ to be determined. (There is no loss of generality in adopting this choice of t_α as opposed to letting the denominator of (4.23) be a general function of ϵ.) The various time-scales can then be expressed in terms of t_α:

$$t = t_0 + \epsilon^{\alpha - 1} t_\alpha; \quad \tilde{t} = \tilde{t}_0 + \epsilon^\alpha t_\alpha, \tag{4.24a, b}$$

$$t^+ \equiv \int_0^t F(\epsilon\tau)\, \mathrm{d}\tau = t_0^+ + \epsilon^{\alpha-1} t_\alpha + \tfrac{1}{2}\epsilon^{2\alpha-1} a_1 t_\alpha^2 + \tfrac{1}{3}\epsilon^{3\alpha-1} a_2 t_\alpha^3 + O(\epsilon^{4\alpha-1}), \tag{4.24c}$$

$$t^* = \epsilon^{\alpha - \frac{1}{3}} t_\alpha + \beta_1 \epsilon^{2\alpha - \frac{1}{3}} t_\alpha^2, \tag{4.24d}$$

where we have used the notation

$$t_0^+ = \int_0^{t_0} F(\epsilon\tau)\,\mathrm{d}\tau; \quad t_0 = \frac{\tilde{t}_0}{\epsilon}. \tag{4.24e,f}$$

Consider first the matching condition on ϵS_1 and $\epsilon^{\frac{1}{2}} S_1^*$ along the $\bar{\xi}^* = \text{const.}$ characteristics, i.e.

$$\lim_{\substack{\epsilon\to 0\\ t_\alpha \text{fixed}}} \frac{1}{\epsilon^{\frac{1}{2}}}\left\{\epsilon S_1\left(x, \frac{\tilde{t}_0}{\epsilon}+\epsilon^{\alpha-1}t_\alpha, \tilde{t}_0+\epsilon^\alpha t_\alpha; 0\right) - \epsilon^{\frac{1}{2}} S_1^*\left(x, \frac{\tilde{t}_0}{\epsilon}+\epsilon^{\alpha-1}t_\alpha, \epsilon^{\alpha-\frac{1}{2}}t_\alpha+\beta_1\epsilon^{2\alpha-\frac{1}{2}}t_\alpha^2; 0\right)\right\} = 0. \tag{4.25}$$

Since S_1 is not singular as $\tilde{t}\to\tilde{t}_0$, $\epsilon S_1/\epsilon^{\frac{1}{2}} = O(\epsilon^{\frac{1}{2}})\to 0$ as $\epsilon\to 0$, with t_α fixed. Therefore, we must set $S_1^* = 0$ in this limit, and this just gives the trivial solution: $f_1^*(\zeta, t^*; 0) = 0$. With this result, the argument of Φ^* as given by (4.19*a*) is $x - 2t - \frac{1}{2}a_1 t^{*2}$. Thus, using (4.24*a*, *d*) we see that in the matching domain the characteristics associated with f_1^* are the curves

$$x - 2\epsilon^{\alpha-1}t_\alpha - \tfrac{1}{2}a_1(\epsilon^{2\alpha-1}t_\alpha^2 + 2\beta_1\epsilon^{3\alpha-1}t_\alpha^3) + O(\epsilon^{4\alpha-1}) = c_5 + 2t_0 = \text{const.} \tag{4.26a}$$

The curves $\bar{\xi}^* = \text{const.}$ associated with the precritical solution for S_1 have the following form when we use (4.24) in (4.9*a*):

$$x - 2\epsilon^{\alpha-1}t_\alpha - \tfrac{1}{2}a_1\epsilon^{2\alpha-1}t_\alpha^2 - \tfrac{1}{3}\alpha_2\epsilon^{3\alpha-1}t_\alpha^3 + O(\epsilon^{4\alpha-1}) = \bar{\xi}^* + t_0^+ + t_0 = \text{const.} \tag{4.26b}$$

Matching (4.26*a*) with (4.26*b*) to $O(\epsilon^{\frac{1}{2}})$ gives

$$\beta_1 = \frac{a_2}{3a_1}; \quad c_5 = \bar{\xi}^* + t_0^+ - t_0, \tag{4.27a,b}$$

and the $O(\epsilon^{4\alpha-1})$-remainder term divided by $\epsilon^{\frac{1}{2}}$ vanishes if $\alpha > \frac{3}{8}$. We shall demonstrate that this condition defines the lower bound of the overlap domain.

Next we consider the matching of ϵR_1 with $\epsilon^{\frac{1}{2}} R_1^*$ along the $\bar{\eta}^* = \text{const.}$ characteristics. We must have

$$\lim_{\substack{\epsilon\to 0\\ t_\alpha \text{fixed}}} \frac{1}{\epsilon^{\frac{1}{2}}}\left\{\epsilon R_1\left(x, \frac{\tilde{t}_0}{\epsilon}+\epsilon^{\alpha-1}t_\alpha, \tilde{t}_0+\epsilon^\alpha t_\alpha; 0\right) - \epsilon^{\frac{1}{2}} R_1^*\left(x, \frac{\tilde{t}_0}{\epsilon}+\epsilon^{\alpha-1}t_\alpha, \epsilon^{\alpha-\frac{1}{2}}t_\alpha+\frac{a_2}{3a_1}\epsilon^{2\alpha-\frac{1}{2}}t_\alpha^2; 0\right)\right\} = 0, \tag{4.28}$$

where we have used (4.27*a*) for β_1. Using (4.10*b*), we find

$$\frac{\epsilon R_1}{\epsilon^{\frac{1}{2}}} = \frac{B(x)}{a_1 t_\alpha}\epsilon^{\frac{1}{2}-\alpha} + O(\epsilon^{\frac{1}{2}}) \quad \text{as} \quad \epsilon\to 0, \quad t_\alpha \text{ fixed}. \tag{4.29}$$

The dominant term on the right-hand side of (4.29) arises entirely from the singular term $\epsilon B(x)/[F(\tilde{t})-1]$ in R_1. In the matching to $O(\epsilon^{\frac{1}{2}})$ this term vanishes in the overlap domain since $\alpha < \frac{1}{2}$ by definition in (4.23). Therefore, we must also have $R_1^* = 0$. This does not mean that the singular term in (4.10*b*) may be ignored; in the matching to $O(\epsilon)$ it becomes $O(\epsilon^{-\alpha})$ and can only be matched with a corresponding term in the $O(\epsilon^{\frac{1}{2}})$ transcritical solution. To demonstrate this, note that in the matching to $O(\epsilon)$ we must multiply (4.29) by $\epsilon^{-\frac{1}{2}}$. The dominant term on the right-hand side then becomes $B(x)/a_1\epsilon^\alpha t_\alpha$ and will therefore be singular for any $\alpha > 0$ if $B(x) \neq 0$. Moreover, when written in terms of t^* this term is just $\epsilon^{\frac{1}{2}}B(x)/a_1 t^*$, which means that it can only be matched with a corresponding term in the $O(\epsilon^{\frac{1}{2}})$ contribution of the transcritical

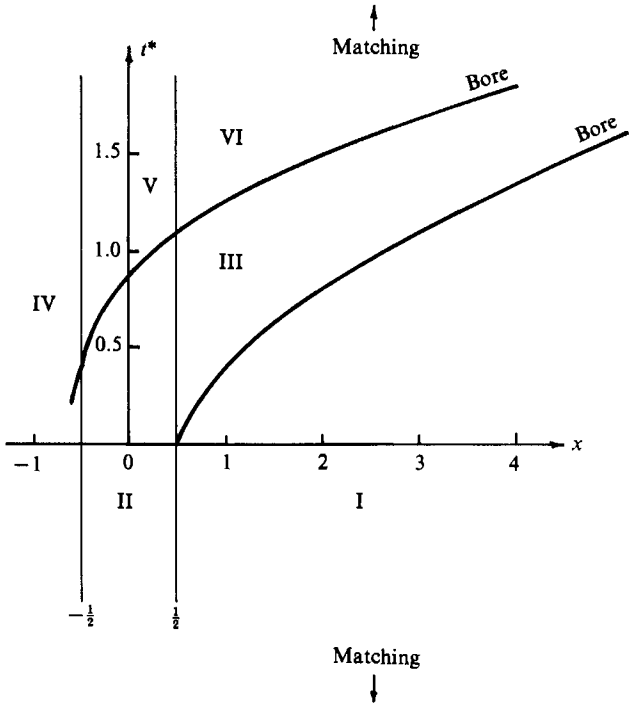

FIGURE 9. Critical solution domains.

expansion. Once we have determined this expansion completely we shall demonstrate that the solution in $|x| \leqslant \frac{1}{2}$, where $B(x) \neq 0$, does indeed have such a term.

The result $R_1^* = 0$ in the matching region means that $g_1^* \to 0$ as $t^* \to -\infty$, and (4.19*b*) implies that

$$w \to a_1 t^* \quad \text{as} \quad t^* \to -\infty. \tag{4.30}$$

Now, in the matching region the curves $\bar{\eta}^* = \text{const.}$, defined by (4.9*b*), have the behaviour

$$x - \tfrac{1}{2}\epsilon^{2\alpha-1} a_1 t_\alpha^2 - \tfrac{1}{3}\epsilon^{3\alpha-1} a_2 t_\alpha^3 + O(\epsilon^{4\alpha-1}) = \bar{\eta}^* + t_0^+ - t_0 = \text{const.} \tag{4.31}$$

We must show that the characteristics of (4.16*b*) (with $\kappa^* = 0$) have the same behaviour. To fix ideas, consider the case $a_1 > 0$. Because $\mathrm{d}x/\mathrm{d}t^* = w \to a_1 t^*$ along a characteristic as $t^* \to -\infty$, we will always have $x > \frac{1}{2}$ in this limit, i.e. matching occurs in the lower-right region, $x > \frac{1}{2}, t^* \to -\infty$ indicated in figure 9 and we must use (4.21) for the solution and the characteristic curves in this case. With use of (4.27*a*) we have $w = a_1 \epsilon^{\alpha-1/2} t_\alpha + \frac{1}{3} a_2 \epsilon^{2\alpha-1/2} t_\alpha^2$, i.e. $c_3 = 0$, and

$$x - \tfrac{1}{2} a_1 \left(t_\alpha^2 \epsilon^{2\alpha-1} + \frac{2a_2}{3a_1} \epsilon^{3\alpha-1} t_\alpha^3 \right) + O(\epsilon^{4\alpha-1}) = -\frac{c_4}{2a_1} = \text{const.}, \tag{4.32}$$

which is in agreement with (4.31) to $O(\epsilon^{\frac{1}{2}})$ as long as $\alpha > \frac{3}{8}$. In effect, the matching of characteristics determines the constant c_4 in terms of the constants associated with the precritical solution in the form $c_4 = 2a_1(t_0 - t_0^+ - \bar{\eta}^*)$. A similar calculation confirms the matching of characteristics for the case $a_1 < 0$. This concludes the matching to $O(\epsilon^{\frac{1}{2}})$ and exhibits the overlap domain to be defined by $\frac{3}{8} < \alpha < \frac{1}{2}$.

We show next that the information obtained by the matching in the lower right of the (x, t^*)-plane allows us to calculate the explicit form of the transcritical solution everywhere else, and we again concentrate on the case $a_1 > 0$. In particular, we shall

show that the (x, t^*)-plane is subdivided into the six regions bounded by the vertical lines $x = \pm\frac{1}{2}$ and the two bores indicated in figure 9.

As pointed out earlier, matching occurs as $t^* \to -\infty$ in what has been labelled region I. Since the asymptotic form of (4.21*a*) as $t^* \to -\infty$ is just w itself, the matching determines w in all of region I to be

$$w = a_1 t^*, \quad \text{on} \quad x - \tfrac{1}{2}a_1 t^{*2} = x_0 = \text{const.}, \tag{4.33a, b}$$

where $x_0 = \bar{\eta}^* + t_0^+ - t_0$ is the value of x when $t^* = 0$. In particular, at any point along the vertical line $x = \frac{1}{2}, t^* = t_0^* \leqslant 0$, we have $w = a_1 t_0^*$, and we now use this condition to determine the two constants c_1, c_2 in (4.20) for the solution in region II. We find

$$w^2 = (a_1 t_0^*)^2 - a_1 + 2a_1 x - \tfrac{3}{2}B(x), \tag{4.34a}$$

along the curves

$$\left(x + \tfrac{1}{6}a_1 + \frac{w}{\sqrt{6}}\right)e^{-\sqrt{6}t^*} = \left(\tfrac{1}{2} + \tfrac{1}{6}a_1 + \frac{a_1 t_0^*}{\sqrt{6}}\right)e^{-\sqrt{6}t_0^*}. \tag{4.34b}$$

This can be simplified to read

$$w = \sqrt{6}(\tfrac{1}{2} + \tfrac{1}{6}a_1)\sinh\sqrt{6}(t^* - t_0^*) + a_1 t_0^* \cosh\sqrt{6}(t^* - t_0^*), \tag{4.34c}$$

along

$$x = -\tfrac{1}{6}a_1 + (\tfrac{1}{2} + \tfrac{1}{6}a_1)\cosh\sqrt{6}(t^* - t_0^*) + \frac{a_1 t_0^*}{\sqrt{6}}\sinh\sqrt{6}(t^* - t_0^*). \tag{4.34d}$$

We are now in a position to demonstrate the matching of the singular term $\epsilon B(x)/[F(\tilde{t}) - 1]$ with a corresponding term in (4.34). Solving (4.34*b*) for $t^* - t_0^*$, then using (4.34*a*) to eliminate w gives

$$t^* - t_0^* = \frac{1}{\sqrt{6}}\log\frac{6x + a_1 - [6(a_1 t_0^*)^2 - 6a_1 + 12a_1 x - 9B(x)]^{\frac{1}{2}}}{3 + a_1 + \sqrt{6}a_1 t_0^*}. \tag{4.35}$$

In the matching for region II, we have x fixed: $|x| \leqslant \frac{1}{2}$ and $t^* \to -\infty$. Expanding (4.35) in this limit shows that $t_0^* \to -\infty$ also, and that

$$t^* - t_0^* = \frac{x - \frac{1}{2}}{a_1 t^*} + O(t^{*-3}) \quad \text{as } t^* \to -\infty. \tag{4.36}$$

Since $t^* - t_0^* \to 0$, we can expand (4.34*d*) to obtain

$$x = \tfrac{1}{2} + \tfrac{1}{2}a_1 t^{*2} - \tfrac{1}{2}a_1 t_0^{*2} + O(t_0^{*-2}), \tag{4.37}$$

and using this in (4.34*a*) gives

$$w = -[(a_1 t^*)^2 - \tfrac{3}{2}B(x) + O(t^{*-2})]^{\frac{1}{2}} \quad \text{as } t^* \to -\infty, \tag{4.38a}$$

or

$$w = a_1 t^* - \frac{3}{4}\frac{B(x)}{a_1 t^*} + O(t^{*-3}) \quad \text{as } t^* \to -\infty. \tag{4.38b}$$

Therefore, using (4.22*b*) and (4.19*b*) we have

$$\epsilon^{\frac{1}{2}}R_1^* = \frac{\epsilon^{\frac{1}{2}}B(x)}{a_1 t^*} + O(\epsilon^{\frac{1}{2}}t^{*-3}). \tag{4.39}$$

Now, in the matching to $O(\epsilon)$, the singular part of ϵR_1 matches identically with the dominant term in (4.39), and the $O(\epsilon^{\frac{1}{2}}t^{*-3})$-term when divided by ϵ becomes $O(\epsilon^{1-3\alpha})$ and will match with a singular term proportional to $\epsilon^2/(F-1)^3$ in the precritical expansion to $O(\epsilon^2)$.

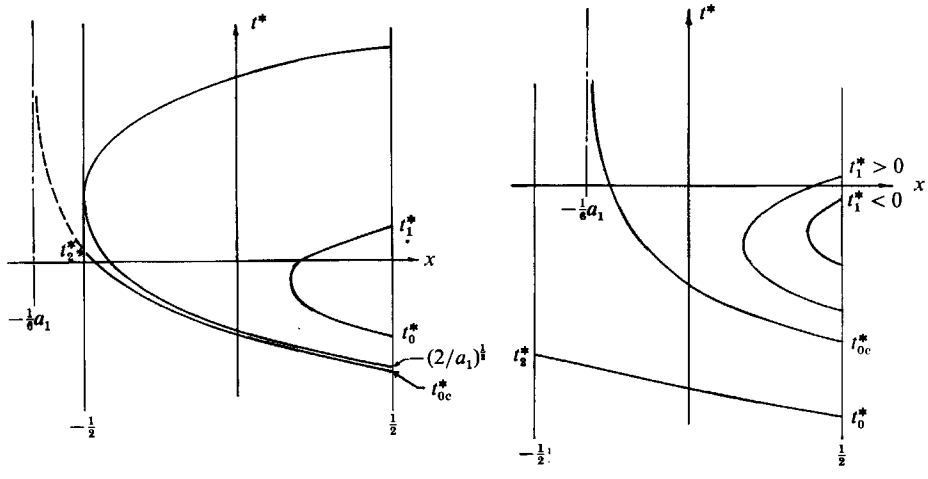

FIGURE 10. (*a*) Characteristics in $|x| \leqslant \frac{1}{2}$ for $a_1 = 4$, (*b*) $a_1 = 2$.

We now resume our calculation of the remainder of the transcritical solution, and note that the characteristics (4.34*d*) have the following geometric property. The curve on which

$$t_0^* = -\frac{3+a_1}{\sqrt{6a_1}} \equiv t_{0c}^*,$$

approaches the vertical asymptote $x = -\frac{1}{6}a_1$ as $t^* \to \infty$. This asymptote lies to the left of $x = -\frac{1}{2}$ if $a_1 > 3$ and to the right if $a_1 \leqslant 3$, as distinguished in figures 10*a* and 10*b*. The family of curves originating from $x = \frac{1}{2}, t^* = t_0^* \leqslant 0$ splits into two subfamilies. The members of the first group arrive at $x = \frac{1}{2}, t^* = t_1^*$, while the remainder terminate at $x = -\frac{1}{2}, t^* = t_2^*$ (see figure 10). We calculate t_1^* by setting $x = \frac{1}{2}$ in (4.34*b*) and find

$$t_1^* \equiv t_0^* + \frac{1}{\sqrt{6}} \log \frac{3+a_1-\sqrt{6a_1}\,t_0^*}{3+a_1+\sqrt{6a_1}\,t_0^*}. \tag{4.40}$$

The above holds for all t_0^* in the range $-(2/a_1)^{\frac{1}{2}} \leqslant t_0^* \leqslant 0$ if $a_1 > 3$, and all t_0^* in the range $t_{0c}^* < t_0^* \leqslant 0$ if $a_1 \leqslant 3$. It is also easy to show that t_1^* is always positive if $a_1 > 3$ and t_1^* may be negative for sufficiently small t_0^* if $a_1 \leqslant 3$. To calculate t_2^* we set $x = -\frac{1}{2}$ in (4.34*b*) and obtain the expression

$$t_2^* \equiv t_0^* + \frac{1}{\sqrt{6}} \log \frac{3+a_1-\sqrt{6a_1}\,t_0^*}{-3+a_1+(6a_1^2 t_0^{*2}-12a_1)^{\frac{1}{2}}}, \tag{4.41}$$

which may be positive or negative. It is valid for all t_0^* in the range $-\infty < t_0^* < -(2/a_1)^{\frac{1}{2}}$ if $a_1 > 3$ and $-\infty < t_0^* < t_{0c}^*$ if $a_1 \leqslant 3$.

To calculate the solution in III, we use (4.34) on $x = \frac{1}{2}, t^* = t_1^*$ to evaluate the two arbitrary constants c_3 and c_4 in (4.21). The result is

$$w = a_1(t^*-t_1^*) - a_1 t_0^*, \tag{4.42a}$$

along the curves

$$x = \tfrac{1}{2} + (t^*-t_1^*)\,[\tfrac{1}{2}a_1(t^*-t_1^*) - a_1 t_0^*]. \tag{4.42b}$$

In a similar manner, we calculate the solution in IV to be

$$w = a_1(t^*-t_2^*)-(a_1^2 t_0^{*2}-2a_1)^{\frac{1}{2}}, \tag{4.43a}$$

along the curves

$$x = -\tfrac{1}{2}+(t^*-t_2^*)\,[\tfrac{1}{2}a_1(t^*-t_2^*)-(a_1^2 t_0^{*2}-2a_1)^{\frac{1}{2}}]. \tag{4.43b}$$

We now use the information given by the above solution on $x = -\frac{1}{2}$ to obtain the solution in V as follows:

$$w = [(a_1 t_0^*)^2 - a_1 + 2a_1 x - \tfrac{3}{2}B(x)]^{\frac{1}{2}}, \tag{4.44a}$$

along the curves

$$\left(x+\tfrac{1}{6}a_1+\frac{w}{\sqrt{6}}\right)e^{-\sqrt{6}t^*} = \left(-\tfrac{1}{2}+\tfrac{1}{6}a_1+\frac{[(a_1 t_0^*)^2-2a_1]^{\frac{1}{2}}}{\sqrt{6}}\right)e^{-\sqrt{6}t_3^*}, \tag{4.44b}$$

or,

$$w = \sqrt{6}(\tfrac{1}{6}a_1-\tfrac{1}{2})\sinh\sqrt{6}(t^*-t_3^*)+(a_1^2 t_0^{*2}-2a_1)^{\frac{1}{2}}\cosh\sqrt{6}(t^*-t_3^*), \tag{4.44c}$$

along the curves

$$x = -\tfrac{1}{6}a_1+(\tfrac{1}{6}a_1-\tfrac{1}{2})\cosh\sqrt{6}(t^*-t_3^*)+[\tfrac{1}{6}(a_1^2 t_0^{*2}-2a_1)]^{\frac{1}{2}}\sinh\sqrt{6}(t^*-t_3^*), \tag{4.44d}$$

where

$$t_3^* \equiv t_2^*+\frac{2}{a_1}(a_1^2 t_0^{*2}-2a_1)^{\frac{1}{2}}. \tag{4.45}$$

Finally, we connect region VI to region V to obtain

$$w = a_1(t^*-t_4^*)-a_1 t_0^*, \tag{4.46a}$$

along the curves

$$x = \tfrac{1}{2}+\tfrac{1}{2}(t^*-t_4^*)\,[a_1(t^*-t_4^*)-2a_1 t_0^*], \tag{4.46b}$$

where

$$t_4^* \equiv t_3^*+\frac{1}{\sqrt{6}}\log\frac{3+a_1-\sqrt{6}a_1 t_0^*}{-3+a_1+(6a_1^2 t_0^{*2}-12a_1)^{\frac{1}{2}}}. \tag{4.47}$$

Consider now the two bores displayed in figure 9. It follows from the solution in region II that one bore starts at the fixed point

$$t^* = 0; \quad x = \tfrac{1}{2} \tag{4.48a, b}$$

if $a_1 \geqslant 3$, and at the point with coordinates defined by

$$t^* = t_s^*+\frac{1}{2\sqrt{6}}\log\frac{\sqrt{6}-2a_1 t_s^*}{\sqrt{6}+2a_1 t_s^*}, \tag{4.49a}$$

$$x = -\tfrac{1}{6}a_1+(\tfrac{1}{2}+\tfrac{1}{6}a_1)\cosh\sqrt{6}(t^*-t_s^*)+\frac{a_1 t_s^*}{\sqrt{6}}\sinh\sqrt{6}(t^*-t_s^*), \tag{4.49b}$$

with

$$t_s^* \equiv -\frac{1}{2a_1}(6-2a_1)^{\frac{1}{2}}, \tag{4.49c}$$

if $a_1 < 3$.

To analyse the second bore which starts near $x = -\frac{1}{2}$, we use the solution defined in IV and obtain the following parametric form for the envelope of characteristics:

$$t^* = t_2^*+\frac{\mathrm{d}t_2^*}{\mathrm{d}t_0^*}(a_1^2 t_0^{*2}-2a_1)^{\frac{1}{2}}\Big/\left[a_1\frac{\mathrm{d}t_2^*}{\mathrm{d}t_0^*}+\frac{a_1^2 t_0^*}{(a_1^2 t_0^{*2}-2a_1)^{\frac{1}{2}}}\right], \tag{4.50a}$$

$$x = -\tfrac{1}{2}+\tfrac{1}{2}(t^*-t_2^*)\,[a_1(t^*-t_2^*)-(4a_1^2 t_0^{*2}-8a_1)^{\frac{1}{2}}], \tag{4.50b}$$

and t_2^* is defined in (4.41). For a given a_1, this system can be solved numerically to minimize t^* with respect to t_0^* to obtain the starting point for the bore. For example, if $a_1 = 4$, we find $x = -0.5055$ and $t^* = 0.2691$.

The jump condition across these two bores is the same as that given by (3.24) of §3.2, i.e.

$$C^* = \epsilon^{\frac{1}{2}} \frac{\mathrm{d}x}{\mathrm{d}t^*} = \epsilon^{\frac{1}{2}}[a_1 t^* - \tfrac{3}{8}(g_1^{*+} + g_1^{*-})] + O(\epsilon), \tag{4.51a}$$

which corresponds to the following divergence form for w:

$$w_{t^*} + (\tfrac{1}{2}w^2)_x = a_1 - \tfrac{3}{4}B_x. \tag{4.51b}$$

The behaviour of the solution, including bores in the transcritical region, will be exhibited in §4.4 where it is compared with numerical results.

4.3. *Postcritical expansion; matching*, ($\kappa^* = 0$)

We have shown that passage through the value $F = 1$ introduces disturbances which have an $O(\epsilon^{\frac{1}{2}})$ amplitude and depend explicitly on the slow scale $t^* = \epsilon^{\frac{1}{2}}t$ that is not present in the precritical solution. Therefore, for $(\tilde{t} - \tilde{t}_0) \gg \epsilon^{\frac{1}{2}}$, the expansion must proceed in powers of $\epsilon^{\frac{1}{2}}$ and involve the slow scales $\epsilon^{i/2}t$, $i = 1, 2, \ldots$. Again, the results that are known in the transcritical region allow us to match only to $O(\epsilon^{\frac{1}{2}})$ so we can define the postcritical solution only to this order. Moreover, we can only determine the dependence of the $O(\epsilon^{\frac{1}{2}})$-solution on the slow scale t^*; the dependence of this solution on the slower scales requires knowledge of the higher-order terms.

We proceed as in the precritical region by solving the problem in the coordinates of (2.8), then transform the results to the coordinates in (2.11) in order to carry out the matching. The solution has the form

$$u(x, t; \epsilon, 0) = F(\tilde{t}) + \epsilon^{\frac{1}{2}}\hat{u}_1(x, t, t^*) + O(\epsilon), \tag{4.52a}$$

$$h(x, t; \epsilon, 0) = 1 + \epsilon^{\frac{1}{2}}\hat{h}_1(x, t, t^*) + O(\epsilon), \tag{4.52b}$$

The functions $\hat{u}_1$ and $\hat{h}_1$ may be expressed in the characteristic form

$$\hat{u}_1 = \tfrac{1}{2}(\hat{f}_1 - \hat{g}_1); \quad \hat{h}_1 = \tfrac{1}{2}(\hat{f}_1 + \hat{g}_1). \tag{4.53a, b}$$

As before, $\hat{f}_1$ and $\hat{g}_1$ obey evolution equations which can be solved in the form

$$\hat{f}_1 = \hat{\Phi}(x - t^+ - t - \tfrac{3}{4}\hat{f}_1 t^*); \quad \hat{g}_1 = \hat{\Gamma}(x - t^+ + t + \tfrac{3}{4}\hat{g}_1 t^*). \tag{4.54a, b}$$

We now need to determine the functions $\hat{\Phi}$ and $\hat{\Gamma}$ by matching (4.54) with the transcritical solution. The bore originating from the vicinity of $x = -\frac{1}{2}$ intersects the $x = \frac{1}{2}$ line at some time $t^* = O(1)$. Therefore, the matching region, in which $t^* \to \infty$, corresponds to the upper-right domain indicated in figure 9. The reason we need only consider $x \geqslant \frac{1}{2}$ in the matching is that all the characteristics originating in regions IV or V eventually cross the $x \geqslant \frac{1}{2}$ line. Thus, we must match the transcritical solutions in regions I, III and VI with corresponding solutions (4.54).

First, we note that the result $S_1^* = 0$ in the transcritical solution implies that $\Phi = 0$. Thus, we only have a $\hat{g}_1$ contribution to u and h in the postcritical region. Consider now the transcritical solution in region I defined by (4.33). Since $w = a_1 t^*$, we have $g_1^* = 0$ (cf. (4.17)), along the curves $x - \frac{1}{2}a_1 t^{*2} = x_0 = \text{const}$. Matching g_1^* with $\hat{g}_1$ requires that we set $\hat{g}_1 = 0$. In this event, the characteristics in the postcritical region are the curves (cf. (4.54b))

$$x - t^+ + t = \text{const}. \tag{4.55}$$

Using the same definition (4.23) for the matching variable t_α (now $t_\alpha > 0$) shows that

the curves $x-\frac{1}{2}a_1 t^{*2} = \text{const.}$ match with (4.55) in the part of the overlap domain contained in I.

Matching the solutions in III gives

$$\hat{g}_1 = \text{const.} = \tfrac{4}{3}a_1(t_0^* + t_1^*), \tag{4.56a}$$

along $$x - t^+ + t + a_1(t_0^* + t_1^*)\,t^* = \text{const.}$$

$$= -t_0^+ + t_0 + \tfrac{1}{2} + \tfrac{1}{2}a_1 t_1^{*2} + a_1 t_0^* t_1^*. \tag{4.56b}$$

Using (4.24) in (4.56*b*) gives the following expression valid in the matching region:

$$x - \tfrac{1}{2}a_1 t^{*2} + a_1(t_0^* + t_1^*)\,t^* + O(\epsilon^{4\alpha-1}) = \tfrac{1}{2} + \tfrac{1}{2}a_1 t_1^{*2} + a_1 t_0^* t_1^*, \tag{4.57}$$

which agrees with (4.42*b*).

It remains to match the solutions in region VI. We find

$$\hat{g}_1 = \text{const.} = \tfrac{4}{3}a_1(t_0^* + t_4^*), \tag{4.58a}$$

along $$x - t^+ + t + a_1(t_0^* + t_4^*)\,t^* = \text{const.}$$

$$= -t_0^+ + t_0 + \tfrac{1}{2} + \tfrac{1}{2}a_1 t_4^{*2} + a_1 t_0^* t_4^*. \tag{4.58b}$$

Using (4.24), (4.58*b*) takes the form

$$x - \tfrac{1}{2}a_1 t^{*2} + a_1(t_0^* + t_4^*)\,t^* + O(\epsilon^{4\alpha-1}) = \tfrac{1}{2} + \tfrac{1}{2}a_1 t_4^{*2} + a_1 t_0^* t_4^*, \tag{4.59}$$

which agrees with (4.46*b*).

This completes the matching of the transcritical and postcritical solutions to $O(\epsilon^{\frac{1}{2}})$ in the overlap domain $\frac{3}{8} < \alpha < \frac{1}{2}$. We find that the singular term $B(x)/[F(\tilde{t})-1]$ also occurs in the postcritical expansion for R to $O(\epsilon)$. As in the case of the precritical solution, one can show that this term will now match with a corresponding term of the transcritical solution in region V. The bore condition for the postcritical solution is

$$\frac{\mathrm{d}\hat{\eta}}{\mathrm{d}t^*} = -\tfrac{3}{8}(\hat{g}_1^+ + \hat{g}_1^-). \tag{4.60}$$

Therefore, the correct divergence form for the evolution equation governing $\hat{g}_1$ is

$$(\hat{g}_1)_{t^*} + (-\tfrac{3}{8}\hat{g}_1^2)_{\hat{\eta}} = 0, \tag{4.61}$$

with $\hat{\eta} = x - t^+ + t$. Since $g_1^* = \hat{g}_1$ in the matching, it is easily seen that bores in the transcritical region with speed C^*, as given by (4.51*a*), match with the bores defined above.

4.4. *Discussion and numerical verification of results*

To illustrate the preceding results, we study the simple linear case

$$F(\tilde{t}) = 0.3 + 3.2\tilde{t}. \tag{4.62}$$

A second example problem where F varies nonlinearly with $\tilde{t}$ is given in Yu (1988). Here, $F(0) = 0.3, \tilde{t} = 0.21875, a_1 = 3.2, a_2 = 0$, and in the numerical results that are shown next, we have taken $\epsilon = 0.1$. The two bores displayed in figure 9 are calculated for the above case and start at the points $x = \frac{1}{2}, t^* = 0$ and $x = -0.5192, t^* = 0.3488$. These bores continue to propagate into the postcritical region and determine an interval in x over which the dominant disturbance is to be found.

In figure 11 we show the boundaries of the disturbances in the (x,t)-plane. In the precritical region we again have three disturbances of order ϵ consisting of a stationary disturbance bounded by $|x| = \pm\frac{1}{2}$, the f-wave bounded by $\bar{\xi}^* = \pm\frac{1}{2}$ and

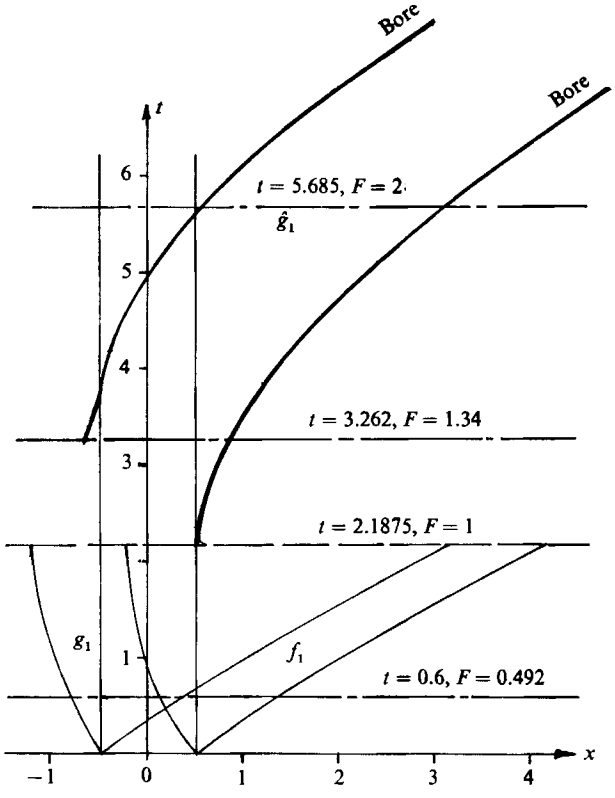

FIGURE 11. Solution domains and bores for $F = 0.3+3.2\tilde{t}, \epsilon = 0.1$.

propagating downstream, and the g-wave bounded by $\bar{\eta}^* = \pm\frac{1}{2}$. The g-wave initially propagates upstream but as F increases, it decelerates and reverses direction to interact with the stationary disturbance. The interaction occurs in the transcritical region and gives rise to an $O(\epsilon^{\frac{1}{2}})$ N-wave which is the dominant part of the solution when $(F-1) \gg \epsilon^{\frac{1}{2}}$. This N-wave is bounded by the two bores which originated in the transcritical region. In addition, we have the stationary disturbance and the continuation of the f-wave, both of which being $O(\epsilon)$ have not been computed in our postcritical solution.

In figure 12, we exhibit the theoretical results (dashed curves) for h at the times $t = 0.6$, 2.1875, 3.262 and 5.685, indicated in figure 11. These results are compared with numerical solutions (solid curves) calculated using the algorithm in §3.1. In all these results $\epsilon = 0.1$ and F satisfies (4.62).

For $t = 0.6$ $(F = 0.492, F^* = -1.61, t^* = -0.5)$ we have used the precritical solution (4.8b) to calculate the dashed curve. We find that the maximum error is 2.3×10^{-2} which is consistent for an $O(\epsilon)$-theory with $\epsilon = 0.1$. The f-wave is discernible as the depression in h at the right; the stationary disturbance is the dominant central depression which has combined with the g-wave on the left.

For $t = 2.1875$ $(F = 1, F^* = 0, t^* = 0)$ we use the transcritical solution and, as seen from figure 11, the f-wave is just to the right of the calculation range and does not appear in the numerical results. This time corresponds to the x-axis of figure 9. Thus, the bore at $x = \frac{1}{2}$ has just emerged. To the right of this bore the solution is zero, and to its left the solution is in region II and given by (4.34) up to $x = -\frac{1}{2}$. At this point,

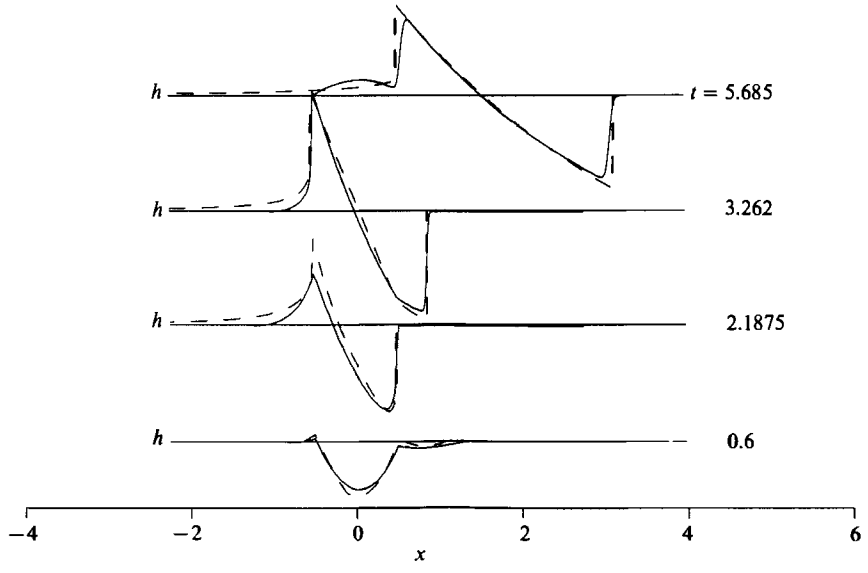

FIGURE 12. Free surface at various t for $\epsilon = 0.1, F = 0.3 + 3.2\tilde{t}$. The solid curve shows the numerical result.

we encounter the discontinuity in slope as we switch over to the solution in region IV for $x < -\frac{1}{2}$ (see figure 9). The maximum error for this time is $0.7 \times 10^{-1} = O(\epsilon)$ and is consistent with an $O(\epsilon^{\frac{1}{2}})$-theory.

For $t = 3.262$ $(F = 1.34, F^* = 1.08, t^* = 0.34)$, $(F-1)/\epsilon^{\frac{1}{2}} = 1.1 = O(1)$. Hence we still use the transcritical solution. As indicated in figure 11, the left bore has just emerged at this time and both bores are well defined in our results. The maximum error for this case is $1.7 \times 10^{-1} = O(\epsilon)$ and occurs near the right bore. The error near the left bore is 0.03 and the maximum error away from the bores is 0.02.

The top curve illustrates the postcritical solution. Here $t = 5.685$, i.e. $F = 2.12$ and $(F-1)/\epsilon^{\frac{1}{2}} = 3.54$ which may be regarded as large (note that for $\epsilon = 0.1, \epsilon^{\frac{1}{2}} = 0.316$, therefore a factor of three may be regarded as large). Now, we find a well defined N-wave that is accurately described by our results of §4.3; the maximum error is 2.0×10^{-1} and occurs near both bores. These errors are entirely due to the errors in the bore location. The maximum error for the bore location is $0.8 \times 10^{-1} = O(\epsilon)$ and occurs at the left bore. This is consistent with our $O(\epsilon^{\frac{1}{2}})$ theory. In the numerical result we note, in addition, the $O(\epsilon)$-stationary disturbance over the interval $|x| < \frac{1}{2}$ that we have not calculated. (We also have not calculated the $O(\epsilon)$ f-wave which is beyond the right boundary of this figure.)

In conclusion, we have demonstrated the accuracy of our asymptotic theory to the orders worked out for the simple linear variation in F as defined in (4.62). More detail comparisons, including examples with $a_2 \neq 0$ can be found in Yu (1988). The principal result of this analysis is that as F passes through the critical value, disturbances of order-ϵ amplify to form an N-wave having an $O(\epsilon^{\frac{1}{2}})$-amplitude and slowly increasing wavelength.

The authors would like to express their grateful thanks to the National Science Foundation, who supported the project under the Grant No. DMS-8606198.

REFERENCES

AKYLAS, T. R. 1984 *J. Fluid Mech.* **141**, 455–466.

COLE. S. L. 1983 *Q. Appl. Maths* **41**, 301–309.

COLE, S. L. 1985 *Wave Motion* **7**, 579–587.

COPELAND, B. 1977 A description of a Fourier method for Korteweg–de Vries type equations. *Tech. Rep. 77–2*, The Institute of Applied Mathematics and Statistics, University of British Columbia, Vancouver, B.C.

FRENZEN, C. L. 1982 Multiple variable expansions for interacting weakly nonlinear waves; applications to shallow water surface waves with variable mean shear and bottom topography. Ph.D thesis, University of Washington, Seattle, WA.

FRENZEN, C. L. & KEVORKIAN, J. 1985 *Wave Motion* **7**, 25–42.

GRIMSHAW, R. H. J. & SMYTH, N. 1986 *J. Fluid Mech.* **169**, 429–464.

HOUGHTON, D. D. & KASAHARA, A. 1968 *Comm. on Pure and Appl. Math.* **21**, 1–23.

KEVORKIAN, J. 1982 *Stud. Appl. Maths* **66**, 95–119.

KEVORKIAN, J. 1987 *SIAM Rev.* **29**, 391–461.

KEVORKIAN, J. & COLE, J. D. 1981 *Perturbation Methods in Applied Mathematics.* Springer.

MAINARDI, F. & LEBLOND, P. H. 1987 In *Proc. Intl Conf. on the Applications of Multiple Scaling in Mechanics*, pp. 239–245. Paris: Masson.

MEI, C. C. 1986 *J. Fluid Mech.* **162**, 53–67.

MELVILLE, W. K. & HELFRICH, K. R. 1987 *J. Fluid Mech.* **178**, 31–57.

MILES, J. W. 1986 *J. Fluid Mech.* **162**, 489–499.

SMYTH, N. F. 1987 *Proc. R. Soc. Lond.* A **409**, 79–97.

STOKER, J. J. 1957 *Water Waves.* Interscience.

WHITHAM, G. B. 1974 *Linear and Nonlinear Waves.* Wiley-Interscience.

WU, T. Y. 1987 *J. Fluid Mech.* **184**, 75–99.

YU, J. 1988 Passage through the critical Froude number for shallow water waves over a variable bottom. Ph.D. thesis, University of Washington, Seattle, WA.